



HAL
open science

Application of Mathematical Epidemiology to crop vector-borne diseases. The cassava mosaic virus disease case

Michael Chapwanya, Yves Dumont

► **To cite this version:**

Michael Chapwanya, Yves Dumont. Application of Mathematical Epidemiology to crop vector-borne diseases. The cassava mosaic virus disease case. Miranda I. Teboh-Ewungkem; Gideon Akumah Ngwa. *Infectious Diseases and our Planet*, 7, Springer, 2021, *Mathematics of Planet Earth*, 978-3-030-50825-8. 10.1007/978-3-030-50826-5_4 . hal-02401399

HAL Id: hal-02401399

<https://hal.science/hal-02401399v1>

Submitted on 9 Dec 2019

HAL is a multi-disciplinary open access archive for the deposit and dissemination of scientific research documents, whether they are published or not. The documents may come from teaching and research institutions in France or abroad, or from public or private research centers.

L'archive ouverte pluridisciplinaire **HAL**, est destinée au dépôt et à la diffusion de documents scientifiques de niveau recherche, publiés ou non, émanant des établissements d'enseignement et de recherche français ou étrangers, des laboratoires publics ou privés.

Application of Mathematical Epidemiology to crop vector-borne diseases. The cassava mosaic virus disease case.

Michael Chapwanya¹ and Yves Dumont^{1,2,3,4 *}

¹University of Pretoria, Department of Mathematics and Applied Mathematics, Pretoria, South Africa

²CIRAD, UMR AMAP, F-34398 Montpellier, France

³AMAP, Univ Montpellier, CIRAD, CNRS, INRA, IRD, Montpellier, France

⁴EPITAG, LIRIMA, France

Abstract

In this chapter, an application of Mathematical Epidemiology to crop vector-borne diseases is presented to investigate the interactions between crops, vectors, and virus. The main illustrative example is the cassava mosaic disease (CMD). The CMD virus has two routes of infection: through vectors and also through infected crops. In the field, the main tool to control CMD spreading is roguing. The presented biological model is sufficiently generic and the same methodology can be adapted to other crops or crop vector-borne diseases. After an introduction where a brief history of crop diseases and useful information on Cassava and CMD is given, we develop and study a compartmental temporal model, taking into account the crop growth and the vector dynamics. A brief qualitative analysis of the model is provided, i.e., existence and uniqueness of a solution, existence of a disease-free equilibrium and existence of an endemic equilibrium. We also provide conditions for local (global) asymptotic stability and show that a Hopf Bifurcation may occur, for instance, when diseased plants are removed. Numerical simulations are provided to illustrate all possible behaviors. Finally, we discuss the theoretical and numerical outputs in terms of crop protection.

1 Introduction

Agriculture began from around 9000 BC independently in different places around the world. Since then, humans have developed their knowledge to produce food more efficiently and to increase crop yields, while promoting the development of the human community. However, this is possible as long as Mother Earth has the capacity to sustain all developments induced by humans. Looking ahead to the year 2050, approximately 9 billion people are expected to live in places where 10 000 years ago, only a few hundred thousands were living. In essence, there is a challenge to provide food for people on (more and more) limited area of (arable) land. Even if crop yields have drastically increased during the last century, crops have to face new dangers in the form of diseases and pests. For a number of years, pesticides were developed as a solution to combat the spread of pests and diseases. Unfortunately, we now know that most of these pesticides have caused a lot of damage (like cancer, lost in the biodiversity, etc). Consequently, there is need to develop sustainable approaches to maintain yields and reduce the use of chemical products as much as possible in order to protect the biodiversity, decrease the risk of cancer or other diseases, and, also, to protect our Earth for the future generations.

While the first mathematical model on inoculation against smallpox was developed by Daniel Bernoulli around 1760, it is mostly acknowledged that Mathematical Epidemiology and the first compartmental models were initiated, not by mathematicians, but by public health physicians, like Sir R.A. Ross, W.H. Hamer, A.G. McKendrick, and W.O. Kermack between 1900 and 1935, [7] (see also [4]). Since then, various epidemiological models have been developed and studied mathematically.

*Corresponding author: yves.dumont@cirad.fr

However, while mathematical models for vector borne diseases in humans and animals are well documented in the literature, very little work has been done in modeling vector-borne diseases in plants.

The aim of this chapter is to present an example of crop-vector-virus interaction, using cassava crop because it has become a very important crop for many people in Africa. After rice and maize, it is now the third-largest source of food and carbohydrates, [18]. We will begin here in the introduction by giving a brief historical background of crop diseases to emphasize that crop diseases are as old as human diseases like malaria, and probably started with the neolithic revolution when humans moved from a lifestyle of hunting and gathering to one of agriculture and settlement. We then explain the importance of cassava and the impact of its main disease, the cassava mosaic disease, and summarize previous modeling works.

1.1 Crop diseases in the past

Crop diseases are known since the ancient time (see for instance [33] and also [5]). Plant diseases have been recorded in a few Egyptian writings, on Sumerian clay tablets (1200 BC), and also in the Old Testament and in the Talmud. Even in the far East, plant diseases were recognized, in particular, in India, Vedic literature (1500-500 BC), and also some two thousands old works are available in China. In ancient Greece, some diseases of trees, cereals and vegetables have been reported by Theophrastus (371-287 BC), also known as the 'father of Botany'. He was student, collaborator and successor of Aristotle. Theophrastus and Pliny the Elder (23 -79 AD), became the references in Europe until the end of the Middle Age. However, between the 8th and 13th century, the Arab agricultural revolution occurred. Ibn al-Awwam (Seville, late 12th) wrote one of the most important medieval book on Agriculture and also about the symptoms of tree and vine diseases as well as (more or less realistic) methods to cure. Aztec, Inca and Mayas in the Americas also faced diseases on maize and potatoes, that will be imported by conquistadors, first, in Spain and in Portugal (in 1493, for maize, when Christopher Columbus went back to Spain [21]; potatoes were only recorded in the literature in 1537 after the Spaniards discovered high Andes of South America [23]), before their spreading throughout Europe along the 16th -17th centuries. They became major crops in many countries in the "Old World". Particularly potatoes, leading to one of the most notable historical impacts of plant disease, the Irish potato famine of 1845, that was caused by late blight fungus, *Phytophthora infestans*. Approximately one million people perished from starvation; around one million and a half more are believed to have left Ireland and immigrated to the United States. The French vine industry was devastated in 1878 by another fungal pathogen, the powdery mildew. This is the first time where disease management was able to find a solution and produce the first fungicide ever, the Bordeaux mixture (made with copper sulfate and lime mixture). However, for the vine industry, the real disaster came with the phylloxera, a sap sucking insects, that first devastated most of the vineyards in the continent before spreading to the rest of the world, except some places, like Chile. In fact, the number of diseases (and also pest attacks) have increased dramatically since the 19th century, with the increase in population mobility and also with the increase of trade exchanges, including the importation of alien plants/plant products containing diseases or insects (vectors of diseases). What is unusual with crop vector-borne diseases is that in general one vector (aphids for instance) is able to transmit several to hundreds of viruses on many crops. So that several crops can be impacted on at the same time by several virus causing more damages and eventually death. Since the discoveries of new lands, the importation of new crops, the increase of trades and population displacements, diseases and vectors have invaded or are invading areas where plants are fully susceptible, such that, in the recent decades, pests and diseases have become a major problem in many crops around the world, and, especially in Africa.

1.2 About cassava, cassava mosaic disease, and its vector

This chapter focuses on cassava (*Manihot esculenta* Crantz) and the cassava mosaic virus. Cassava was domesticated in the southwestern Amazon of Brazil and Bolivia some 8,000-10,000 years ago (see [26] for further details). It was introduced from the Americas onto Africa by Portuguese traders in the 16th century. Since then it has spread on the African continent, such that, after rice and corn, it has become a very important staple food for over 500 millions people in Africa alone. Cassava can

grow in places where other crops cannot. It is tolerant to drought and can grow on soils with a low nutrient capacity. Cassava is a perennial crop. However the storage roots can be harvested from 6 to 24 months after planting, depending on the cultivar and the growing conditions. Moreover, the roots can be left in the ground without harvesting for a long period of time, making it a very useful crop as a security against famine. That is why cassava is considered as a food security crop. Its study and its protection against bio-aggressors are of main importance. The current average yields per hectare is around 12.5 tonnes, while the optimal yields can be as high as 80 tonnes under optimal conditions. This shows that there is potential for increase in production. More than 1 million of small-scale farmers around the world are producing cassava. See [14] for further information.

Cassava mosaic geminiviruses (CMGs) are the causal agents of cassava mosaic disease (CMD), which is one of the most widespread and devastating diseases of cassava in Africa. For instance, in the 1990s a severe form of the CMD lead to yield losses of 80 to 100 percent in Uganda and Kenya (FAO, 2015). Currently, nine distinct CMG species (seven African and two Indian) have been found to infect cassava [41].

CMD is now prevalent in many parts of Africa [43]. The geminiviruses and their whitefly vector (*Bemisia tabaci*) have been studied extensively and much attention has been given to possible control measures and their deployment since the 1990s. CMD was first described in Tanzania in 1894. Till then, CMD became prevalent in most of the countries of sub-Saharan Africa due to the continuous cultivation of susceptible cultivars and the indiscriminate use of diseased propagation material. As highlighted in [25] (an references therein), CMD is also propagated routinely from stem cuttings coming from infected plants, such that the virus can be maintained within the plant waiting for vectors to spread. Early studies found that some varieties of cassava were less affected than others by CMD, so that resistance programs were launched in the 1930s-1940s. In the 1980s and 1990s, many projects aimed at controlling CMD were launched in Kenya, Ivory Coast and Uganda, such that CMD received more attention than any other crop disease and this also explains why CMD is always so prominent in the literature on cassava. However, whatever the research efforts done in the last thirty years, CMD is still a problem.

Cassava mosaic geminiviruses are transmitted in a persistent manner by whiteflies, *B. tabaci* (see [34] for a recent review). This was first showed in 1932 in the Democratic Republic of Congo. Further studies showed that whiteflies are the sole vectors. There are some vectors that can acquire the virus but are unable to transmit it. The minimum time between acquisition and becoming infected is around 7 hours. However, the transmission efficiency is very low (0.15 – 1.7% for insect collected in the field [15], to moderate (4 – 13%) for laboratory-reared insects [36]. The CMGs spreading is mainly related to the susceptibility/resistance of the cassava varieties, the phytosanitation measures and if CMGs are systemic within the infected plants. However, clearly, the mobility of the whiteflies is a key factor and in general higher incidence due to severe CMD is mainly due to a high level of infestation by *B. tabaci*. Last but not least *B. tabaci* also causes direct damages to cassava by feeding on phloem or deposition of honeydew, which acts as a substrate for sooty moulds (a black, non-parasitic, superficial growth of fungi on plant surfaces), that reduces both respiration and photosynthesis [39]. Surprisingly, as highlighted in [34], the research effort on the ecology of these insects was very little compared to all work done on the virus and resistant cassava cultivars. However, *B. tabaci* is a polyphagous herbivore that can potentially use a wide range of different host plants (more than 500) in cassava production landscape so that, in general, intercropping cassava with other plants (maize, coffee, sweet potato, bean, etc) may result in a lower *B. tabaci* population abundance. However, the mechanisms resulting in the decay are not necessarily related to host-preference. Coming back to the biology of *B. tabaci*, published information suggests that its development period from egg to adult emergence is between 19 and 29 days, and the species goes through four nymphal instars before entering a pupal phase. However, in this paper, we will not enter in such details since we mainly focus on *B. tabaci* as vector of the CMD. Note also that *B. tabaci* is able to transmit more than 150 viruses, such that it has become a very serious pest, not only for cassava. In particular, another virus that is really detrimental to cassava, also transmitted by *B. tabaci*, is the cassava brown streak virus (CBSV) [32].

The symptoms of CMD are very well known. Common symptoms include misshapen leaves, chlorosis, mottling and mosaic. Less severe symptoms are ill-defined mosaic patterns, green mosaic with slight or absence of leaf distortion. Thus, in general, symptoms range from barely perceptible mosaic to stunting and general decline of plants. The more severe the symptoms, the lower the yield.

In general young plants are more severely infected than old ones. Last but not least, the symptoms are even more severe in the case of co-infection by two cassava strains, like ACMV (African Cassava Mosaic Virus) and EACMV (Eastern-Africa Cassava Mosaic Virus). There is a synergistic interaction between the two viruses.

Since the early CMD epidemics, phytosanitary strategies have been developed. Of course, these control strategies should be sustainable, and preferably with no use of pesticides. Following [43], three approaches to decrease losses due to a virus disease have been proposed:

- (i) decrease the proportion of infected plants;
- (ii) delay infection to such a late stage of crop growth so that losses become unimportant;
- (iii) decrease the severity of damage sustained after infection in diverse ways.

These objectives can be achieved using phytosanitation, disease-resistant varieties, good cultural practices, vector-control and mild-strain protection. All previous control measures, combined or not, have been more or less studied. In this work, we will particularly explore roguing (the removal of diseased/infected plants), that is a very well known means of virus disease control. It is now clear that whiteflies are not easy to control by insecticides, such that vector control seems to be ineffective. However, we will also explore other control approaches that are used by small-scale farmers for other crops against whiteflies that are not necessarily used to protect cassava.

1.3 On the usefulness of Mathematical Modeling of cassava mosaic disease

The previous summary on Cassava and Cassava Mosaic Virus shows that despite years of study, field investigations and field experiments, the risk of severe epidemics like in the 1990's cannot be excluded. We believe it is not enough to launch new research programs based only on field experiments/observations and laboratory experiments. We need to consider additional tools such as mathematical modeling and computer simulations. Mathematical modeling offers a cheaper, convenient and powerful tool to explore the Cassava-CMD system and go further in order to better understand the possible dynamics that can occur and to possibly point out new ways worth investigating. Some mathematical models on CMD have already been developed, see for instance [17, 25, 27], but they were mostly studied using numerical simulations, without providing the qualitative analysis of the proposed mathematical models. Of course, here we distinguish compartmental models from statistical models, which are, in general, based on data sets. The paper from Holt et al. [25] provides many interesting results. However their models are mainly based on the fact that *B. tabaci* population is limited by cassava individuals, which, in an African context, is not really true since in the introduction, we emphasize that the host range for *B. tabaci* is large and that in general cassava is inter-cropped with other plants. Thus the vector-population is modeled using a logistic-like equation in the susceptible compartment, assuming some kind of skip-oviposition in the birth-rate functional, but this is not clearly explained. They also assumed constant replanting and additional mortality rate for infected plants. Both crop and vector interact using mass-action principle. Since, it has been highlighted that *B. tabaci* population size can be very large, the use of a simple mass-action function could be questionable: in fact it is not the case here since the vector population is limited by the number of cassava individuals (which is a restriction, as explained above). However, the reader has to be aware that this is the way the modeling works: you consider and/or give modeling assumptions to build your model(s), such that for the same biological problem you can derive many different models, see for example the discussion in [28]. Using their models [25], Holt and collaborators obtained various results, mainly based on numerical simulations. Their study showed a range of dynamic behavior including cycles of infection. In their conclusions, clearly selection the cuttings and roguing are the main tools to lower the incidence of the disease. In [48] and more recently in [24], authors included vector aggregation (and also dispersal in [24]) in their models, through nonlinear acquisition and inoculation rates. These previous works highlight the wide diversity and complexity of plant-vector-virus modeling. However, among all these models and also many others in crop epidemiology, plants are always considered as mature individuals, ignoring their growth and the effect of vectors on them before and during outbreaks [9].

The structure of the chapter is as follows: in section 2, we build the mathematical model related to Cassava-CMVD interactions taking into account plant biomass growth. In section 3, a qualitative

analysis is provided. In section 4, a specific study about the permanence of the disease is done. Finally, in section 5, a sensitivity analysis followed by numerical simulations are given to illustrate the theoretical results. In particular, we discuss the usefulness of roguing and eventually other control options that could be tested with our approach.

2 The mathematical model

The model is formulated by considering two compartments: the total plant biomass P , and the vector population density V . The total biomass is further subdivided into two disjoint epidemiological states: the susceptible healthy biomass H_p , and the infectious biomass I_p , so that $P = H_p + I_p$. Similarly, the vector population is divided into two disjoint analogous classes, the susceptible vectors S_v , and the infectious vector I_v so that $V = S_v + I_v$. Based on the above knowledge, we propose the epidemiological structure represented by the compartmental diagram presented in Fig. 1, page 6, which leads to the following system of equations

$$\begin{cases} \frac{dH_p}{dt} = r_p(V)H_p - m_hPH_p - \beta_{vp}H_pI_v - k_pH_p, \\ \frac{dI_p}{dt} = r_p(V)I_p + \beta_{vp}H_pI_v - m_iPI_p - \gamma I_p - k_pI_p, \\ \frac{dS_v}{dt} = \alpha_v(I_p)V - (\mu_1 + \mu_2V)S_v - \beta_{pv}S_vI_p, \\ \frac{dI_v}{dt} = \beta_{pv}S_vI_p - (\mu_1 + \mu_2V)I_v, \end{cases} \quad (1)$$

with initial conditions

$$H_p(0) = H_p^0 \geq 0, \quad I_p(0) = I_p^0 \geq 0, \quad S_v(0) = S_v^0 \geq 0, \quad I_v(0) = I_v^0 \geq 0,$$

where all the parameters are positive. Let us now describe the formulation of model (1) in detail.

Following [31] (see also [40]), the crop biomass growth is assumed to be a nonlinear process, influenced by maintenance (respiration, etc) and intra-specific competition, while the biomass production (through photosynthesis, reproduction, etc) is assumed to be a linear process of the biomass. Thus, the total biomass P follows a logistic-like equation

$$\frac{dP}{dt} = (r_p(V) - k_p)P - m_h(P)P,$$

where $r_p(V)$ is the biomass production rate, k_p is the harvest rate, and the function $m_h(P)$ represents the losses of biomass due to respiration, transpiration and maintenance. It is a positive increasing function of the biomass [31]. According to [29], where the authors fit cassava (dry) biomass growth with a logistic equation, we set $m_h(P) = m_hP$. Our crop growth model is very "simple" compared to previous process-based models (PBM) (like for instance GUMCAS [37], GUMCAS-DSSAT [19], and SIMANIHOT [42]), but sufficient to explore the dynamics of the disease, while keeping the model mathematically tractable. Last but not least, the use of the previous PBM needs to estimate all the physiological parameters not only on healthy plants but also on diseased plants. These data are in general never available.

The function $r_p(V)$ is assumed to be a decreasing and bounded function of V , i.e., $r_p'(V) \leq 0$. This makes sense since the increase in the vector population may negatively impact the production of new biomass.

According to whiteflies biology, and like in [9], we assume that the vector population follows a logistic growth with $\alpha_v - \mu_1$ being the net growth rate, and μ_2 being the death rate due to the density effect. Contrary to [25], we don't rely the dynamics on the presence/absence of cassava, since in the African context, many other cultivated crops can host whiteflies. In fact, we follow [27], where the authors revisited the Holt Cassava Model by considering a logistic equation to model the whiteflies dynamic. However, we take into account that whiteflies have a negative effect on Cassava growth rate, such that the growth rate function is decreasing with increasing V , through a parameter ϕ , related to sap sucking. We also assume that all vector newborns are susceptible and, according to the mean

lifespan of whiteflies, we assume that all infected vectors stay infected for the rest of their lives (the impact of the viruliferous period can be very important within a spatio-temporal model [9]).

The presence of the virus in the host and in the vector populations has several effects. We model only two known effects that were not necessarily developed in previous models:

- (i) First, infected plants grow less than susceptible plants: the maintenance of the infected biomass, m_i , is larger than m_h , the maintenance parameter of healthy plant, due to plant defences mechanisms.
- (ii) Second, the vector growth rate, $\alpha_v - \mu_1$, can also be impacted positively by the presence of diseased plants (see [10]), so that we consider $\alpha_v(I_p) - \mu_1$.

Infection between the plants and vectors is modelled by the mass-action principle. The parameter β_{vp} represents the contact rate between infectious vectors and susceptible plants. Similarly, β_{pv} represents the contact rate between infectious plants and susceptible vectors. The assumption is that the environment is uniform, homogeneous and randomly mixed. In the model we also introduce the roguing parameter γ , i.e., the rate at which infected biomass is removed. In addition, k_p is the rate at which the cassava is harvested for their tuberous roots. The model assumes both the susceptible and infected biomass can be harvested. A summary (and values) of all parameters is provided in Table 1, page 7. Detailed explanations of the given range of values is provided at the beginning of section 5, page 17.

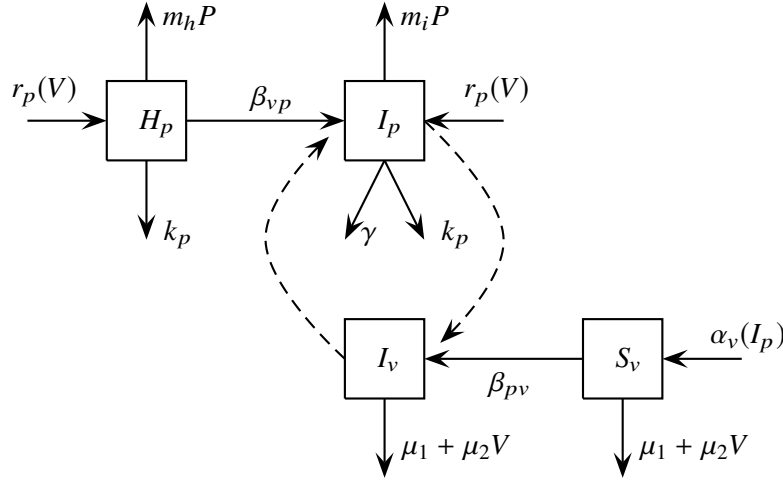


Figure 1: Schematic diagram of the model.

Following (1), when CMV is circulating, P and V satisfy the following equations

$$\frac{dP}{dt} = (r_p(V) - k_p)P - (m_h H_p + m_i I_p)P - \gamma I_p, \quad (2)$$

and

$$\frac{dV}{dt} = \alpha_v(I_p)V - (\mu_1 + \mu_2 V)V. \quad (3)$$

3 Qualitative analysis

In this section we take $r_p(V) = r/(1 + \phi V)$, which satisfies the assumption above for $\phi, r > 0$ with $r_p(V) \leq r_p(0) = r$. In addition, a possible choice for α_v is $\alpha_v(I_p) = \alpha \left(1 + \frac{\delta I_p}{1 + I_p}\right)$ which satisfies $\alpha'_v(I_p) > 0$ and $\alpha \leq \alpha_v(I_p) \leq \alpha(1 + \delta)$ for all I_p . We start with the well-posedness result which we state as follows.

Parameters	Name	Range	Unit	Source
r	biomass maximal growth rate	[0.01, 0.06]	day ⁻¹	estimated from [29]
ϕ	impact of sap sucking per vector	[0, 0.02]	vector ⁻¹	assumed
m_h	maintenance rate per unit of biomass	[0.003, 0.01]	biomass ⁻¹ day ⁻¹	estimated from [29]
$m_i \geq m_h$	maintenance rate per unit of biomass when the biomass is infected	[0.01, 0.1]	biomass ⁻¹ day ⁻¹	assumed
β_{vp}	infection rate	[0.002, 0.032]	vector ⁻¹ day ⁻¹	[25]
γ	roguing rate	[0, 1]	day ⁻¹	assumed
α	whitefly rate of increase	[0.1, 1]	day ⁻¹	estimated from [27]
μ_1	average death rate	[0.05, 0.2]	day ⁻¹	estimated from [27]
μ_2	average density death rate	[0.0001, 0.01]	vector ⁻¹ day ⁻¹	estimated from [27]
β_{pv}	acquisition rate	[0.01, 0.1]	biomass ⁻¹ day ⁻¹	assumed
k_p	mean harvest rate	[0.0025, 0.0072]	day ⁻¹	estimated from [25]
δ	boost parameter related to I_p	[0, 1]	-	assumed

Table 1: Range of values for the parameters of system (1).

Theorem 3.1 Assume $\alpha_v(0) > \mu_1$ and $r_p(0) > k_p$. The system defines a dynamical system on the biologically feasible region

$$\Omega = \{(H_p, I_p, S_v, I_v) \in \mathbb{R}_+^4 : H_p + I_p \leq P^\dagger, S_v + I_v \leq V^\dagger\}$$

where $V^\dagger = \frac{\alpha(1+\delta) - \mu_1}{\mu_2}$ and $P^\dagger = \frac{r_p(0) - k_p}{m_h}$.

Proof : We want to show that for any non negative initial data, the system possesses for all $t \geq 0$, a unique solution which lies in the region Ω . We will provide the proof in two steps.

First we want to show that Ω is a positively invariant set. In particular, we want to show that no trajectory leaves Ω by crossing one of its faces, [6]. On the contrary, let us assume there exist $t_1 > 0$ such that $H_p(t_1) = 0$, $H'_p(t_1) < 0$ with $H_p(t) > 0$, $I_p(t) > 0$, $S_v(t) > 0$, $I_v(t) > 0$ for all $t \in (0, t_1)$. The first equation gives

$$\frac{dH_p(t_1)}{dt} = 0,$$

which is a contradiction. Therefore $H_p(t) \geq 0$ for all $t \geq 0$. Similarly for $t_2 > 0$ with $I_p(t_2) = 0$, $I'_p(t_2) < 0$ with $H_p(t) > 0$, $S_v(t) > 0$, $I_v(t) > 0$ for all $t \in (0, t_2)$, we have

$$\frac{dI_p(t_2)}{dt} = \beta_{vp} H_p I_v > 0,$$

and $t_3 > 0$ with $S_v(t_3) = 0$, $S'_v(t_3) < 0$ with $H_p(t) > 0$, $I_p(t) > 0$, $I_v(t) > 0$ for all $t \in (0, t_3)$, we have

$$\frac{dS_v(t_3)}{dt} = \alpha_v(I_p) I_v > 0,$$

and $t_4 > 0$ with $I_v(t_4) = 0$, $I'_v(t_4) < 0$ with $H_p(t) > 0$, $I_p(t) > 0$, $S_v(t) > 0$ for all $t \in (0, t_4)$, we have

$$\frac{dI_v(t_4)}{dt} = \beta_{pv} S_v I_p > 0.$$

Therefore, in all cases the solution remains in Ω for any initial data in Ω .

In the second step, we use the a priori estimate derived below together with the fact that the right-hand side of the system is a locally Lipschitz function.

From equation (2), assuming $I_p \geq 0$ we have the inequality

$$\frac{dP}{dt} \leq (r_p(V) - k_p) - P(m_h H_p + m_i I_p) \leq (r_p(0) - k_p) - m_h P^2,$$

so that $\limsup_{t \rightarrow \infty} P(t) \leq \frac{r_p(0) - k_p}{m_h}$, where we have used the assumption that $r_p(V) > k_p$. Similarly, from equation (3) we have $\limsup_{t \rightarrow \infty} V(t) \leq \frac{\alpha(1 + \delta) - \mu_1}{\mu_2}$ provided $\alpha_v(0) > \mu_1$. That is all the solutions are uniformly bounded. Combining the above two steps we conclude that (1) defines a dynamical system on Ω .

□

3.1 Computation of \mathcal{R}_0

In this section we use the next generation matrix approach described in [45] (see also [12]), to compute the basic reproduction number \mathcal{R}_0 , of the system. In our case, this is defined as the number of secondary infections that an infectious crop or vector could produce when introduced in a healthy population.

The system (1) has a disease-free equilibrium $E_{DFE} = (P^*, 0, V^*, 0)$. We consider only the equations where the infection progress, namely

$$\frac{dX}{dt} = \mathcal{F}(X) - \mathcal{V}(X), \quad (4)$$

where, in this case $X = (I_p, I_v)^t$, and

$$\mathcal{F}(X) = \begin{pmatrix} r_p(V)I_p + \beta_{vp}H_pI_v \\ \beta_{pv}S_vI_p \end{pmatrix} \quad \text{and} \quad \mathcal{V}(X) = \begin{pmatrix} (m_i P + \gamma + k_p)I_p \\ (\mu_1 + \mu_2 V)I_v \end{pmatrix}.$$

Equation (4) distinguishes the rate of appearance of new infections $\mathcal{F}(X)$, from the transfer into or out of the population by any other means, $\mathcal{V}(X)$. Then

$$J_F(X) = \begin{pmatrix} r_p(V) & -r_p^2(V)\phi/rI_p + \beta_{vp}H_p \\ \beta_{pv}S_v & 0 \end{pmatrix}$$

and

$$J_V(X) = \begin{pmatrix} m_i I_p + m_i P + \gamma + k_p & 0 \\ 0 & \mu_1 + \mu_2 V + \mu_2 I_v \end{pmatrix}.$$

We set

$$F = \begin{pmatrix} r_p(V^*) & \beta_{vp}P^* \\ \beta_{pv}V^* & 0 \end{pmatrix}$$

and

$$V = \begin{pmatrix} m_i P^* + \gamma + k_p & 0 \\ 0 & \mu_1 + \mu_2 V^* \end{pmatrix} = \begin{pmatrix} (m_i - m_h)P^* + \gamma + r_p(V^*) & 0 \\ 0 & \alpha_v(0) \end{pmatrix},$$

where $P^* = \frac{r_p(V^*) - k_p}{m_h}$ and $V^* = \frac{\alpha_v(0) - \mu_1}{\mu_2}$. Then the next generation matrix K is

$$FV^{-1} = \begin{pmatrix} r_p(V^*) & \beta_{vp}P^* \\ \beta_{pv}V^* & 0 \end{pmatrix} \begin{pmatrix} \frac{1}{(m_i - m_h)P^* + \gamma + r_p(V^*)} & 0 \\ 0 & \frac{1}{\alpha_v(0)} \end{pmatrix},$$

that is

$$FV^{-1} = \begin{pmatrix} \frac{r_p(V^*)}{(m_i - m_h)P^* + \gamma + r_p(V^*)} & \frac{\beta_{vp}P^*}{\alpha_v(0)} \\ \frac{\beta_{pv}V^*}{(m_i - m_h)P^* + \gamma + r_p(V^*)} & 0 \end{pmatrix}.$$

From which we deduce that

$$\mathcal{R}_0 = \frac{1}{2} \left(\mathcal{V}_0 + \sqrt{\mathcal{V}_0^2 + 4\mathcal{H}_0} \right), \quad (5)$$

where

$$\mathcal{V}_0 = \frac{r_p(V^*)}{(m_i - m_h)P^* + \gamma + r_p(V^*)},$$

represent a vertical transmission (transmission through the production of new plant biomass), and

$$\mathcal{H}_0 = \frac{\beta_{pv}\beta_{vp}V^*P^*}{\alpha_v(0)[(m_i - m_h)P^* + \gamma + r_p(V^*)]} = \frac{\beta_{pv}\beta_{vp}V^*P^*}{\alpha_v(0)[m_iP^* + \gamma + k_p]}$$

represent an horizontal transmission (through vectors)

Remark 3.1 Note also that when $(m_i - m_h)P^* + \gamma = 0$, that is when there is no roguing, i.e., $\gamma = 0$, and $m_i = m_h$, we have $\mathcal{V}_0 = 1$, such that we always have $\mathcal{R}_0 > 1$.

Remark 3.2 Instead of the complex expression given in (5), for the basic reproduction ratio, it would be biologically more natural to consider $\mathcal{V}_0 + \sqrt{\mathcal{H}_0}$, with both ways of transmission: the one-phase infectious process, from plant to plant, and the two-phase infectious process, from vector to plant and from plant to vector. Indeed, $\mathcal{V}_0 + \sqrt{\mathcal{H}_0} < 1$ implies $\mathcal{R}_0 < 1$, and $\mathcal{R}_0 > 1$ implies $\mathcal{V}_0 + \sqrt{\mathcal{H}_0} > 1$.

Finally, following [45], we deduce the following result

Theorem 3.2 When $\mathcal{R}_0 < 1$ the DFE is locally asymptotically stable, while unstable when $\mathcal{R}_0 > 1$.

3.2 Trivial equilibria and their stabilities/unstabilities

Several equilibria exist for model (1). In this section we focus on the following equilibria,

$$E_+ = (0, 0, V^*, 0), \quad E_{++} = (P^\dagger, 0, 0, 0),$$

with $P^\dagger = \frac{r_p(0) - k_p}{m_h} > P^* = \frac{r_p(V^*) - k_p}{m_h}$; the disease-free equilibrium

$$E_{DFE} = (P^*, 0, V^*, 0).$$

Computing the Jacobian of system (1) leads to

$$J = \begin{pmatrix} f(H_p, I_p, S_v, I_v) & -m_h H_p & -\frac{r\phi H_p}{(1+\phi V)^2} & -\frac{r\phi H_p}{(1+\phi V)^2} - \beta_{vp} H_p \\ \beta_{vp} I_v - m_i I_p & g(H_p, I_p, S_v, I_v) & -\frac{r\phi I_p}{(1+\phi V)^2} & -\frac{r\phi I_p}{(1+\phi V)^2} + \beta_{vp} H_p \\ 0 & \alpha'_v(I_p)V - \beta_{pv} S_v & h(H_p, I_p, S_v, I_v) & \alpha_v(I_p) - \mu_2 S_v \\ 0 & \beta_{pv} S_v & \beta_{pv} I_p - \mu_2 I_v & -\mu_2(I_v + V) - \mu_1 \end{pmatrix},$$

where $f(H_p, I_p, S_v, I_v) = r_p(V) - m_h(P + H_p) - \beta_{vp} I_v - k_p$, $g(H_p, I_p, S_v, I_v) = r_p(V) - m_i(P + I_p) - \gamma - k_p$ and $h(H_p, I_p, S_v, I_v) = \alpha_v(I_p) - (\mu_1 + \mu_2 V) - \beta_{pv} I_p - \mu_2 S_v$. Thus at E_+ we have

$$J_{E_+} = \begin{pmatrix} r_p(V^*) - k_p & 0 & 0 & 0 \\ 0 & r_p(V^*) - \gamma - k_p & 0 & 0 \\ 0 & \alpha'_v(0)V^* - \beta_{pv} V^* & -\alpha_v(0) - \mu_2 V^* & \alpha_v(0) - \mu_2 V^* \\ 0 & \beta_{pv} V^* & 0 & -\mu_2 V^* - \mu_1 \end{pmatrix}. \quad (6)$$

Expanding in terms of the first column, it is clear that at least one of the eigenvalues is strictly positive, which implies that E_+ is unstable. At E_{++} we have

$$J_{E_{++}} = \begin{pmatrix} r_p(0) - k_p & -m_h P^\dagger & -r\phi P^\dagger & -P^\dagger(r\phi + 1) \\ 0 & -\gamma - k_p & 0 & \beta_{vp} P^\dagger \\ 0 & 0 & \alpha_v(0) - \mu_1 & \alpha_v(0) \\ 0 & 0 & 0 & -\mu_1 \end{pmatrix}. \quad (7)$$

$J_{E_{++}}$ being an upper triangular matrix, the eigenvalues are the diagonal terms. Since $\alpha_v(0) - \mu_1$ is strictly positive, E_{++} is unstable.

At the disease-free-equilibrium, we have

$$J_{DFE} = \begin{pmatrix} -(r_p(V^*) - k_p) & -m_h P^* & -\frac{\phi P^* r_p^{*2}}{r} & -\frac{\phi P^* r_p^{*2}}{r} - \beta_{vp} P^* \\ 0 & -(m_i - m_h)P^* - \gamma & 0 & \beta_{vp} P^* \\ 0 & \alpha'_v(0) - \beta_{pv} V^* & -\mu_2 V^* & \alpha_v(0) - \mu_2 V^* \\ 0 & \beta_{pv} V^* & 0 & -\mu_2 V^* - \mu_1 \end{pmatrix}.$$

Considering $|J_{DFE} - \lambda I|$, we expand in terms of the first column and this gives $\lambda_1 = -(r_p(V^*) - k_p) < 0$ since $r_p(V^*) > k_p$. We then expand the remaining matrix in terms of the second column and $\lambda_2 = -\mu_2 V^*$. The remaining two eigenvalues are eigenvalues of the matrix

$$\begin{pmatrix} -(m_i - m_h)P^* - \gamma & \beta_{vp} P^* \\ \beta_{pv} V^* & -\mu_1 - \mu_2 V^* \end{pmatrix},$$

or

$$\begin{pmatrix} -((m_i - m_h)P^* + \gamma) & \beta_{vp} P^* \\ \beta_{pv} V^* & -\alpha_v(0) \end{pmatrix}.$$

after applying the definition of P^* and V^* to the diagonal entries of the reduced matrix. Clearly the trace of this matrix is negative and the requirement for positive determinant simplifies to $((m_i - m_h)P^* + \gamma) \alpha_v(0) - \beta_{pv} \beta_{vp} P^* V^* > 0$, that is if

$$\mathcal{J}_0 = \frac{\beta_{pv} \beta_{vp} P^* V^*}{((m_i - m_h)P^* + \gamma) \alpha_v(0)} < 1. \quad (8)$$

We summarize the previous results as follows

Proposition 3.1 Consider model (1):

- The equilibria E_+ and E_{++} are always unstable.
- Assuming $(m_i - m_h)P^* + \gamma > 0$. The disease-free equilibrium, DFE, is locally asymptotically stable when $\mathcal{J}_0 < 1$, and unstable otherwise.

Remark 3.3 When $(m_i - m_h)P^* + \gamma = 0$, according to the previous section, and remark 3.1, page 9, we have $\mathcal{R}_0 > 1$, such that DFE is always unstable.

Remark 3.4 A remark is necessary here with regards to the basic reproduction numbers defined in (5) and (8). They are mathematically equivalent: as indicated in [11] it will depend on the choice of \mathcal{F} . It is however important to have a biologically relevant decomposition. Using the next generation matrix approach, if we choose $r_p(V)I_p$ as part of \mathcal{V} , then $\mathcal{R}_0^2 = \mathcal{J}_0$. However a direct computation shows that since $\mathcal{R}_0 = 1$ so is \mathcal{J}_0 . Indeed, following (5), $\mathcal{R}_0 = 1$ is equivalent to

$$\sqrt{\mathcal{V}_0 + 4\mathcal{H}_0} = 2 - \mathcal{V}_0,$$

or equivalently $\mathcal{H}_0 = 1 - \mathcal{V}_0$, i.e.,

$$\frac{\beta_{pv} \beta_{vp} P^* V^*}{[(m_i - m_h)P^* + \gamma + r_p(V^*)] \alpha_v(0)} = 1 - \frac{r_p(V^*)}{(m_i - m_h)P^* + \gamma + r_p(V^*)},$$

or

$$\frac{\beta_{pv} \beta_{vp} P^* V^*}{\alpha_v(0)} = (m_i - m_h)P^* + \gamma,$$

that is exactly equivalent to have $\mathcal{J}_0 = 1$. More precisely, using the previous result, we can show the following relationships

$$\mathcal{R}_0 \leq \mathcal{J}_0 \leq 1, \quad \text{and} \quad 1 \leq \mathcal{J}_0 \leq \mathcal{R}_0.$$

3.3 Global stability of the DFE

Next we improve on the previous result and show that the disease free equilibrium is globally asymptotically stable (GAS) when $\mathcal{R}_0 \leq 1$. Following the work of [8], we rewrite our system by splitting the uninfected compartments $x = (H_p, S_v)$ from the infected compartments $y = (I_p, I_v)$. That is

$$\begin{cases} \frac{dx}{dt} = f(x, y), \\ \frac{dy}{dt} = g(x, y), \end{cases}$$

such that $g(x, 0) = 0$. Let us consider the system

$$\frac{dx}{dt} = f(x, 0) = \begin{pmatrix} \frac{rH_p}{1 + \phi S_v} - m_h H_p^2 \\ \alpha_v(0)S_v - (\mu_1 + \mu_2 S_v) S_v \end{pmatrix}. \quad (9)$$

The second equation is the well known logistic equation, for which we know that V^* is GAS. Then, we deduce that P^* is GAS for the first equation. Altogether the DFE $x^* = (P^*, V^*)$ is GAS for system (9). Now we consider

$$g(x, y) = \begin{pmatrix} r_p(V)I_p + \beta_{vp}H_pI_v - (m_iP + \gamma + k_p) I_p \\ \beta_{pv}S_vI_p - (\mu_1 + \mu_2V) I_v \end{pmatrix}$$

such that

$$J_g(x, y) = \begin{pmatrix} r_p(V) - (m_iP + m_iI_p + \gamma + k_p) & -\frac{r\phi I_p}{(1 + \phi V)^2} + \beta_{vp}H_p \\ \beta_{pv}S_v & -(\mu_1 + \mu_2V + \mu_2I_v) \end{pmatrix},$$

and

$$J_g(\text{dfe}, 0) = \begin{pmatrix} r_p(V^*) - (m_iP^* + \gamma + k_p) & \beta_{vp}P^* \\ \beta_{pv}V^* & -(\mu_1 + \mu_2V^*) \end{pmatrix}.$$

Then

$$g(x, y) = \begin{pmatrix} -((m_i - m_h)P^* + \gamma) & \beta_{vp}P^* \\ \beta_{pv}V^* & -\alpha_v(0) \end{pmatrix} y - \begin{pmatrix} \beta_{vp}(P^* - H_p) \\ \beta_{pv}(V^* - S_v) \end{pmatrix}.$$

Now we have to show that $\hat{g}(x, y) \geq 0$. This is true if $S_v \leq V^*$ (always verified), and if $H_p \leq P^*$ (always verified).

In addition,

$$A = \begin{pmatrix} -((m_i - m_h)P^* + \gamma) & \beta_{vp}P^* \\ \beta_{pv}V^* & -\alpha_v(0) \end{pmatrix}$$

is a Metzler Matrix. Thus using the result from [8], we have the following result.

Theorem 3.3 *Assume $\gamma + (m_i - m_h)P^* > 0$. The disease-free equilibrium, (DFE) is globally asymptotically stable if $\mathcal{J}_0 \leq 1$ and unstable for $\mathcal{J}_0 > 1$.*

In the next section we investigate the permanence of system (1), page 5, and, potentially, the existence and stability of endemic equilibria.

4 Permanence of system (1) - Endemic equilibrium

Studying the existence (and the stability/instability) of endemic equilibria for system (1) is not an easy task when $\alpha_v(I_p) \equiv \alpha$. However, in Annexe A, page 29, we show that that two types of endemic equilibria may exist (under conditions): a full endemic equilibrium (when the whole biomass is infected, i.e. $H_p = 0$), and an endemic equilibrium (when healthy and infected biomasses co-exist).

Since $\alpha_v(I_p) \geq \alpha_v(0)$, for all $I_p \geq 0$, we would like to show that a direct study is not always necessary and that it is possible to consider the following sub-system of (1) to derive interesting

facts about the dynamics of system (1):

$$\begin{cases} \frac{dH_p}{dt} = r_p(V)H_p - m_h H_p P - \beta_{vp} H_p I_v - k_p H_p, \\ \frac{dI_p}{dt} = r_p(V)I_p + \beta_{vp} H_p I_v - m_i P I_p - \gamma I_p - k_p I_p, \\ \frac{dS_v}{dt} = \alpha_v(0)V - (\mu_1 + \mu_2 V) S_v - \beta_{pv} S_v I_p, \\ \frac{dI_v}{dt} = \beta_{pv} S_v I_p - (\mu_1 + \mu_2 V) I_v, \end{cases} \quad (10)$$

Using the previous results, it is straightforward to show that system (10) admits a unique non negative solution, \underline{x} . Let x be the solution of (1). Then, assuming that $x(0) = \underline{x}(0)$, and using the comparison Theorem (see, for instance, Theorem 3.2, page 209, in [46]), we can deduce that \underline{x} is a lower solution of system (1), that is $x(t) \geq \underline{x}(t)$, for all $t > 0$.

Thus, any sufficient conditions to show permanence of (10), i.e. $\underline{x}(t) > 0$, will ensure permanence of (1), $x(t) > 0$ for all $t > 0$.

Assuming the dynamics of the vector to be very fast compared to the dynamics of the biomass, we assume quasi-steady state approximation such that $V = V^*$. Then, system (10) reduces to

$$\begin{cases} \frac{dH_p}{dt} = r^* H_p - m_h P H_p - \beta_{vp} H_p I_v - k_p H_p, \\ \frac{dI_p}{dt} = r^* I_p + \beta_{vp} H_p I_v - m_i P I_p - \gamma I_p - k_p I_p, \\ \frac{dI_v}{dt} = \beta_{pv}(V^* - I_v)I_p - \alpha_v I_v, \end{cases} \quad (11)$$

where $r^* = r/(1 + \phi V^*)$. For the equilibria we need to solve

$$\begin{aligned} r^* H_p^* - m_h P^* H_p^* - \beta_{vp} H_p^* I_v^* - k_p H_p^* &= 0, \\ r^* I_p^* + \beta_{vp} H_p^* I_v^* - m_i P^* I_p^* - \gamma I_p^* - k_p I_p^* &= 0, \\ \beta_{pv}(V^* - I_v^*)I_p^* - \alpha_v I_v^* &= 0. \end{aligned} \quad (12)$$

Notice that the definition of P^* here is different from earlier results. Thus looking for equilibria in equation (12) leads to

$$(r^* - k_p - m_h H_p - m_i I_p) P^* = \gamma I_p, \quad (13)$$

that is

$$\left(r^* - k_p - m_h P^* - (m_i - m_h) I_p^* \right) P^* = \gamma I_p^*, \quad (14)$$

so that

$$\frac{r^* - k_p - m_h P^*}{(m_i - m_h) P^* + \gamma} P^* = I_p^*, \quad (15)$$

assuming either $\gamma > 0$ or $m_i > m_h$. Thus, if $I_p = 0$ then $P_{\text{dfe}} = \frac{r^* - k_p}{m_h}$, and thus $I_v = 0$ and $H_{p,\text{dfe}} = P_{\text{dfe}}$.

Now assume that $0 \leq \gamma + k_p < r^*$, and $H_p = 0$, then from the second equation and third equation we deduce,

$$P^\# = I_p^\# = \frac{r^* - \gamma - k_p}{m_i}, \quad I_v^\# = \frac{\beta_{pv} P^\#}{\alpha_v + \beta_{pv} P^\#} V^*.$$

The basic reproduction number for the reduced system (11) becomes

$$\mathcal{R}_0 = \frac{1}{2} \left(\frac{r^*}{(m_i - m_h) P_{\text{dfe}} + \gamma + r^*} + \sqrt{\left(\frac{r^*}{(m_i - m_h) P_{\text{dfe}} + \gamma + r^*} \right)^2 + 4 \frac{\beta_{pv} \beta_{vp} P^* V^*}{((m_i - m_h) P_{\text{dfe}} + \gamma + r^*) \alpha_v}} \right).$$

Assume now that $H_p > 0$, Then, using the first equation, we have

$$\frac{r^* - k_p - m_h P^*}{\beta_{vp}} = I_v.$$

Replacing I_v in the third equation leads to

$$\beta_{pv} (V^* - I_v) I_p - \alpha_v I_v = \beta_{pv} \left(V^* - \frac{r^* - k_p - m_h P^*}{\beta_{vp}} \right) I_p - \alpha_v \frac{r^* - k_p - m_h P^*}{\beta_{vp}} = 0.$$

Replacing I_p by $\frac{r^* - k_p - m_h P^*}{(m_i - m_h)P + \gamma} P$ leads to

$$\beta_{pv} \left(V^* - \frac{r^* - k_p - m_h P^*}{\beta_{vp}} \right) \frac{r^* - k_p - m_h P^*}{(m_i - m_h)P^* + \gamma} P^* = \alpha_v \frac{r^* - k_p - m_h P^*}{\beta_{vp}}.$$

Assuming that $(r^* - k_p - m_h P^*) \neq 0$, we can simplify, such that

$$\beta_{pv} (\beta_{vp} V^* - r^* + k_p + m_h P^*) P^* = \alpha_v ((m_i - m_h)P^* + \gamma),$$

that is

$$\beta_{pv} m_h P^{*2} - \beta_{pv} (r^* - k_p - \beta_{vp} V^* - \alpha_v (m_i - m_h)) P^* - \gamma \alpha_v = 0,$$

which is a quadratic equation in P . The discriminant of this equation is

$$\Delta = (\beta_{pv} (r^* - k_p - \beta_{vp} V^*) - \alpha_v (m_i - m_h))^2 + 4\gamma \alpha_v \beta_{pv} m_h > 0,$$

such that there exists only one non-negative solution

$$P^* = \frac{1}{2\beta_{pv} m_h} \left(\beta_{pv} (r^* - k_p - \beta_{vp} V^* - \alpha_v (m_i - m_h)) + \sqrt{\Delta} \right)$$

Then we can deduce

$$I_p^* = \frac{r^* - k_p - m_h P^*}{(m_i - m_h)P^* + \gamma} P^*, \quad H_p = P^* \left(1 - \frac{r^* - k_p - m_h P^*}{(m_i - m_h)P^* + \gamma} \right)$$

and

$$I_v = \frac{r^* - k_p - m_h P^*}{\beta_{vp}}.$$

We summarize the previous results as follows

Proposition 4.1 *System (11) always admits the following three (non zero) equilibria:*

- *The disease free Equilibrium DFE = $(P_{dfe}, 0, 0)$, whatever $\gamma \geq 0$.*
- *When $0 \leq \gamma + k_p < r^*$, a Full Disease Equilibrium, FDE = $(0, P^\#, I_v^\#)$.*
- *When $\gamma > 0$, an endemic equilibrium EE = (H_p^*, I_p^*, I_v^*) .*

One way, to investigate the local (asymptotic) stability, is to compute the Jacobian

$$J(X) = \begin{pmatrix} r^* - k_p - m_h I_p - 2m_h H_p - \beta_{vp} I_v & -m_h H_p & -\beta_{vp} H_p \\ \beta_{vp} I_v - m_i I_p & r^* - m_i P - m_i I_p - \gamma - k_p & \beta_{vp} H_p \\ 0 & \beta_{pv} (V^* - I_v) & -\beta_{pv} I_p - \alpha_v \end{pmatrix} \\ = \begin{pmatrix} r^* - k_p - m_h I_p - 2m_h H_p - \beta_{vp} I_v & -m_h H_p & -\beta_{vp} H_p \\ r^* - k_p - m_h P - m_i I_p & r^* - m_i P - m_i I_p - \gamma - k_p & \beta_{vp} H_p \\ 0 & \beta_{pv} (V^* - I_v) & -\beta_{pv} I_p - \alpha_v \end{pmatrix}.$$

The stability of the disease-free equilibrium follows from the definition of \mathcal{R}_0 . However, in the particular case of $FDE = (0, P^\#, I_v^\#)$, we obtain the following Jacobian Matrix

$$J(FDE) = \begin{pmatrix} r^* - k_p - m_h P^\# - \beta_{vp} V^\# & 0 & 0 \\ r^* - k_p - (m_i + m_h)P^\# & r^* - 2m_i P^\# - \gamma - k_p & 0 \\ 0 & \beta_{pv} (V^* - V^\#) & -(\beta_{pv} P^\# + \alpha_v) \end{pmatrix},$$

that is

$$J(FDE) = \begin{pmatrix} r^* - k_p - m_h \frac{r^* - \gamma - k_p}{m_i} - \beta_{vp} V^\# & 0 & 0 \\ \gamma - m_h P^\# & -r^* + \gamma + k_p & 0 \\ 0 & \beta_{pv} (V^* - V^\#) & -\beta_{pv} P^\# - \alpha_v \end{pmatrix},$$

or

$$J(FDE) = \begin{pmatrix} (r^* - k_p) \left(1 - \frac{m_h}{m_i}\right) + \gamma \frac{m_h}{m_i} - \beta_{vp} V^\# & 0 & 0 \\ \gamma - m_h P^\# & -r^* + \gamma + k_p & 0 \\ 0 & \beta_{pv} (V^* - V^\#) & -\beta_{pv} P^\# - \alpha_v \end{pmatrix},$$

Clearly, the eigenvalues are the terms in the diagonal. They are negative if $\gamma + k_p < r^*$ (this is the condition to have existence of FDE), and $\gamma + P^* (m_i - m_h) < \frac{m_i}{m_h} \beta_{vp} V^\#$. After manipulation, and using (8), the last condition is equivalent to $\mathcal{J}_0 > \frac{P^*}{P^\#} \left(1 + \frac{\beta_{vp} P^\#}{\alpha_v}\right) > 1$. In other words, when \mathcal{J}_0 is sufficiently large, the whole crop can become infected.

Now we consider $EE = (H_p^*, I_p^*, I_v^*)$. We obtain

$$J(EE) = \begin{pmatrix} -m_h H_p^* & -m_h H_p^* & -\beta_{vp} H_p^* \\ r^* - k_p - m_h P^* - m_i I_p & r^* - m_i P^* - m_i I_p - \gamma - k_p & \beta_{vp} H_p^* \\ 0 & \beta_{pv} (V^* - I_v^*) & -\beta_{pv} I_p^* - \alpha_v \end{pmatrix}.$$

In that case, we know that $\gamma + k_p > r^*$, such that the characteristic polynomial becomes

$$p(x) = x^3 + a_2 x^2 + a_1 x + a_0, \quad (16)$$

where, clearly,

$$a_2 = -\text{trace}(J(X^*)) = m_h H_p^* + m_i P^* + m_i I_p^* - r^* + \gamma + k_p + \beta_{pv} I_p^* + \alpha_v > 0.$$

The coefficient a_1 is given by

$$\begin{aligned} a_1 &= \sum_i \sum_{j < i} \begin{vmatrix} a_{ii} & a_{ij} \\ a_{ji} & a_{jj} \end{vmatrix} \\ &= \begin{vmatrix} -m_h H_p^* & -m_h H_p^* \\ r^* - k_p - m_h P^* - m_i I_p & r^* - m_i P^* - m_i I_p - \gamma - k_p \end{vmatrix} + \begin{vmatrix} -m_h H_p & -\beta_{vp} H_p \\ 0 & -\beta_{pv} I_p - \alpha_v \end{vmatrix} \\ &+ \begin{vmatrix} r^* - m_i P^* - m_i I_p - \gamma - k_p & \beta_{vp} H_p \\ \beta_{pv} (V^* - I_v) & -\beta_{pv} I_p - \alpha_v \end{vmatrix}. \end{aligned}$$

It is clear that

$$\begin{aligned} \begin{vmatrix} -m_h H_p^* & -m_h H_p^* \\ r^* - k_p - m_h P^* - m_i I_p^* & r^* - m_i P^* - m_i I_p - \gamma - k_p \end{vmatrix} &= m H_p^* ((m_i - m_h) P^* + \gamma) > 0, \\ \begin{vmatrix} -m_h H_p & -\beta_{vp} \\ 0 & -\beta_{pv} I_p - \alpha_v \end{vmatrix} &= m_h H_p^* (\beta_{pv} I_p + \alpha_v) > 0, \end{aligned}$$

and

$$\begin{aligned} \begin{vmatrix} r^* - m_i P^* - m_i I_p - \gamma - k_p & \beta_{vp} H_p^* \\ \beta_{pv} (V^* - I_v) & -\beta_{pv} I_p - \alpha_v \end{vmatrix} \\ = (m_i P^* + m_i I_p + \gamma + k_p - r^*) (\beta_{pv} I_p^* + \alpha_v) - \beta_{pv} \beta_{vp} H_p^* (V^* - I_v^*). \end{aligned}$$

However, from (12), page 12 we have

$$\beta_{pv}\beta_{vp}H_pV^* = (m_iP^* + \gamma - r^* - k_p) (\alpha_v + \beta_{pv}I_p^*)$$

such that

$$\begin{vmatrix} r^* - m_iP^* - m_iI_p - \gamma - k_p & \beta_{vp}H_p^* \\ \beta_{pv}(V^* - I_v) & -\beta_{pv}I_p - \alpha_v \end{vmatrix} = m_iI_p^*(\beta_{pv}I_p^* + \alpha_v) + \beta_{pv}\beta_{vp}H_p^*I_v^* > 0.$$

In fact

$$a_1 = m_hH_p^*((m_i - m_h)P^* + \gamma) + (m_hH_p^* + m_iI_p^*)(\beta_{pv}I_p^* + \alpha_v) + \beta_{pv}\beta_{vp}H_p^*I_v^* > 0.$$

Thus we deduce that $a_1 > 0$. Finally

$$\begin{aligned} a_0 &= - \begin{vmatrix} -m_hH_p & -m_hH_p & -\beta_{vp}H_p \\ r^* - k_p - m_hP^* - m_iI_p^* & r^* - m_iP^* - m_iI_p - \gamma - k_p & \beta_{vp}H_p \\ 0 & \beta_{pv}(V^* - I_v) & -\beta_{pv}I_p - \alpha_v \end{vmatrix} \\ &= m_hH_p^* \begin{vmatrix} r^* - m_iP^* - m_iI_p - \gamma - k_p & \beta_{vp}H_p \\ \beta_{pv}(V^* - I_v) & -\beta_{pv}I_p - \alpha_v \end{vmatrix} \\ &\quad + \begin{vmatrix} r^* - k_p - m_hP^* - m_iI_p^* & \beta_{pv}(V^* - I_v) & -\beta_{pv}I_p - \alpha_v \\ -mH_p & -\beta_{vp}H_p & \end{vmatrix}. \end{aligned}$$

We have, as given above,

$$\begin{aligned} &m_hH_p^* \begin{vmatrix} r^* - m_iP^* - m_iI_p - \gamma - k_p & \beta_{vp}H_p \\ \beta_{pv}(V^* - I_v) & -\beta_{pv}I_p - \alpha_v \end{vmatrix} \\ &= m_hH_p^* (m_iI_p^*(\beta_{pv}I_p^* + \alpha_v) + \beta_{vp}H_p^*\beta_{pv}I_v^*) > 0, \end{aligned}$$

and

$$\begin{aligned} &\begin{vmatrix} r^* - k_p - m_hP^* - m_iI_p^* & \beta_{pv}(V^* - I_v) & -\beta_{pv}I_p - \alpha_v \\ -m_hH_p & -\beta_{vp}H_p & \end{vmatrix} \\ &= - (m_hP^* + m_iI_p^* - r^* + k_p) (\beta_{pv}\beta_{vp}H_p(V^* - I_v) + m_hH_p^*(\beta_{pv}I_p + \alpha_v)), \end{aligned}$$

with

$$\begin{aligned} &m_hH_p^* (m_iI_p^*(\beta_{pv}I_p^* + \alpha_v)) - (m_hP^* + m_iI_p^* - r^* + k_p) m_hH_p^*(\beta_{pv}I_p + \alpha_v) \\ &= - (m_hP^* - r^* + k_p) m_hH_p^*(\beta_{pv}I_p + \alpha_v) \end{aligned}$$

such that

$$\begin{aligned} a_0 &= m_hH_p^*\beta_{vp}H_p^*\beta_{pv}I_v^* - (m_hP^* - r^* + k_p) m_hH_p^*(\beta_{pv}I_p + \alpha_v) \\ &\quad - (m_hP^* + m_iI_p^* - r^* + k_p) \beta_{pv}\beta_{vp}H_p(V^* - I_v) \end{aligned}$$

$$\begin{aligned} a_0 &= \beta_{pv}\beta_{vp}H_pI_v (m_hH_p^* + m_hP^* + m_iI_p^* - r^* + k_p) - (m_hP^* - r^* + k_p) m_hH_p^*(\beta_{pv}I_p + \alpha_v) \\ &\quad - (m_hP^* + m_iI_p^* - r^* + k_p) \beta_{pv}\beta_{vp}H_pV^* \end{aligned}$$

However, using the fact that

$$r^* - k_p - m_hP^* = \beta_{vp}I_v^*,$$

and

$$H_p^*(\beta_{vp}I_v - m_iI_p) = (m_iI_p + [\gamma + k_p - r^*]) I_p > 0,$$

we have

$$a_0 = \beta_{pv}\beta_{vp}H_p^*I_v^* \left(m_h H_p^* + m_h P^* + m_i I_p^* - r^* + k_p \right) + \beta_{vp}I_v m_h H_p^* (\beta_{pv}I_p + \alpha_v) \\ + \beta_{pv}\beta_{vp}H_p^*V^* \left(\beta_{vp}I_v - m_i I_p^* \right),$$

i.e.,

$$a_0 = \beta_{pv}\beta_{vp}H_p I_v \left(m_h H_p^* + m_h P^* + m_i I_p^* - r^* + k_p \right) + \beta_{vp}I_v m_h H_p^* (\beta_{pv}I_p + \alpha_v) \\ + \beta_{pv}\beta_{vp}V^* (m_i I_p + \gamma - r^* + k_p) I_p > 0$$

Thus the first assumption of Rough-Hurwitz is verified: $a_i > 0$.

We now consider γ , the roguing parameter, as a bifurcation parameter. Let us define

$$\Delta(\gamma) = a_1 a_2 - a_0 \\ = [m_h H_p^* ((m_i - m_h)P^* + \gamma) + (m_h H_p^* + m_i I_p^*)\beta_{pv}I_p^* + \alpha_v] + \beta_{pv}\beta_{vp}H_p^*I_v^* \\ \times [m_h H_p^* + m_i P^* + m_i I_p^* - r^* + \gamma + k_p + \beta_{pv}I_p^* + \alpha_v] \\ - \beta_{pv}\beta_{vp}H_p^*I_v^* \left(m_h H_p^* + m_h P^* + m_i I_p^* - r^* + k_p \right) + \beta_{vp}I_v m_h H_p^* (\beta_{pv}I_p + \alpha_v) \\ + \beta_{pv}\beta_{vp}H_p^*V^* \left(\beta_{vp}I_v - m_i I_p^* \right)$$

In order to show LAS of the endemic equilibrium, we need to show that $\Delta(\gamma) > 0$. However, due to the complexity of the formula, this will be investigated numerically. In addition, it is well known that if $\Delta(\gamma) = 0$ for some values of γ , it means that the polynomial (16) has pure imaginary conjugate roots and one real root. However, it is straightforward to show that this real root is simply $-a_2$ (because $a_1 a_2 - a_0 = 0$).

In fact, if the polynomial defined in (16) has a pair of complex conjugate roots, $a \pm bi$ where $a, b \in \mathbb{R}$, which cross the real axis as γ passes through γ^* , then $\Delta(\gamma)$ changes sign as γ passes through γ^* . This can be showed very easily because we have the following relationship:

$$\Delta(\gamma) = -2a \left(b^2 + r^2 \right) - 2a^3. \quad (17)$$

Similarly, if we assume that $\Delta(\gamma)$ changes sign, then according to the previous formula $a(\gamma)$ will also changes sign too. However, in order to derive a Hopf Bifurcation (see, for instance, Theorem 3.4.2 in [22]), we have an additional property to verify, the so-called "transversality condition" that indicates that the eigenvalues cross the x-axis with a non-zero velocity. In other words

$$\frac{da}{d\gamma}(\gamma^*) = a'(\gamma^*) \neq 0 \quad (18)$$

However, using (17), we have that

$$\Delta'(\gamma_i) = -2a'(\gamma^*)(b^2 + r^2)$$

such that verifying (18) is equivalent to verifying $\Delta'(\gamma^*) \neq 0$. Finally, we deduce that a Hopf Bifurcation related to the roguing parameter γ may occur at (EE, γ^*) if

- there exists a value γ^* such that $\Delta(\gamma^*) = 0$, such the Jacobian J_{EE} has a simple pair of pure imaginary eigenvalues and one real negative eigenvalue, $-a_2$,
- and $\Delta'(\gamma^*) \neq 0$.

In addition, the stability of the periodic solutions is given by the sign of the first Lyapunov coefficient of the dynamics, $l_1(EE, \gamma^*)$. If $l_1(EE, \gamma^*) < 0$ then these solutions are stable limit cycles and the Hopf bifurcation is supercritical, while if $l_1(EE, \gamma^*) > 0$ the Hopf bifurcation is subcritical [30]. l_1 being very difficult to obtain theoretically, we may use MatCont software [13] to estimate it.

We consider the parameters values provided in Table 2, page 17, to illustrate Hopf Bifurcations. These values were chosen thanks to the (range of) values given in Table 1, page 7.

r	ϕ	m_h	m_i	β_{vp}	γ	α_v	μ_1	μ_2	β_{pv}	k_p	δ
0.04	0	0.01	0.01	0.008	[0, 1]	0.2	0.12	0.0002	0.02	0.005	0

Table 2: Parameters values

k_p		H_i	I_p	I_v	γ_i^*	l_1
0.0025	H_2	0.561818	0.097525	3.863322	0.208952	$-2.953532e^{-05}$
	H_1	0.030780	0.113949	4.506589	0.045791	$-1.590897e^{-05}$
0.005	H_2	0.524541	0.090960	3.605623	0.195185	$-3.069432e^{-05}$
	H_1	0.031325	0.106193	4.203102	0.043544	$-1.620631e^{-05}$
0.0072	H_2	0.490470	0.085230	3.380376	0.182667	$-1.659246e^{-05}$
	H_1	0.031934	0.099374	3.935864	0.041605	$-1.659246e^{-03}$

Table 3: Hopf Bifurcation Points coordinates and First Lyapunov coefficient estimate for several harvesting rates (based on Table 1, page 7).

In Table 3, page 17, we present Hopf bifurcation results related to different values of k_p . In fact, it is clear that if $k_p \geq k_p^*$, then there is no Hopf Bifurcation.

To illustrate the Hopf Bifurcation property, we focus on $k_p = 0.005$, in Table 3, when $\delta = 0$, for simplicity. In Fig. 2, page 18, we show the bifurcation analysis of system (11) done with MatCont [13], when $\gamma \in [0.02, 0.12]$: we show that two values, γ_1^* and γ_2^* , exist where a Hopf bifurcation occurs.

However, these two values can be obtained by solving $\Delta(\gamma^*) = 0$. This is illustrated in Figures 3, page 19, and 9, page 25.

Last but not least, since we know that the Hopf bifurcation points are supercritical, we can estimate the periods for different values of $\gamma \in [\gamma_1^*, \gamma_2^*]$, using MatCont. See Fig. 4, page 20. Surprisingly, the period belongs to a large interval, i.e. in [130, 445]. This period might certainly be linked to the crop growth parameters. However, since the period is large, except for values of γ closed from γ_2^* . However, the maximum period, 445 days, is reached at $\gamma = 0.05$. This period is almost 15 months, barely impossible to detect it in the field.

5 Numerical simulations

For the sensitivity analysis and the numerical simulations, we first discuss the parameters values given in Table 1, page 7. Some of them are based on the values used in [29, 25, 27], and some of them are estimated based on the available knowledge on the virus and the cassava crops. In fact, despite so much work and published papers on cassava and CMV, parameter estimation has always been a critical issue. Thus, after carefully checking the literature on cassava and CMD, we have tried to provide "realistic" estimates for all parameters used in our model. It is important to note that here we consider cassava biomass and not individual plants, hence some adjustments to the literature values were necessary.

In fact, it is not easy to get information about cassava growth: among all the work done on cassava, surprisingly, only one study from Australia was found about cassava biomass growth, [29]. These are not exactly the same environmental conditions found in Africa, but in any case, at the plants level, this study shows that a logistic equation can represent well the (dry) biomass growth. We will consider the values obtained in [29] to estimate the range of values of r and m_h . In Africa, the range of planting density can be rather large. However, for the sake of simplicity, we will consider a standard density of 10000 plants per ha, or 1 plant per m^2 .

According to (FAOSTAT2019), the average productivity between 2010 and 2017 is around 9 tons per ha in Africa, this leads to a mean productivity of 0.9 kg per m^2 . Then assuming an harvest index (root weight divided by total plant weight) between 0.5 and 0.7, these leads to a total biomass weight per square meter between 1.3kg and 1.8 kg. Typically, harvest can start 8 months (250 days) after

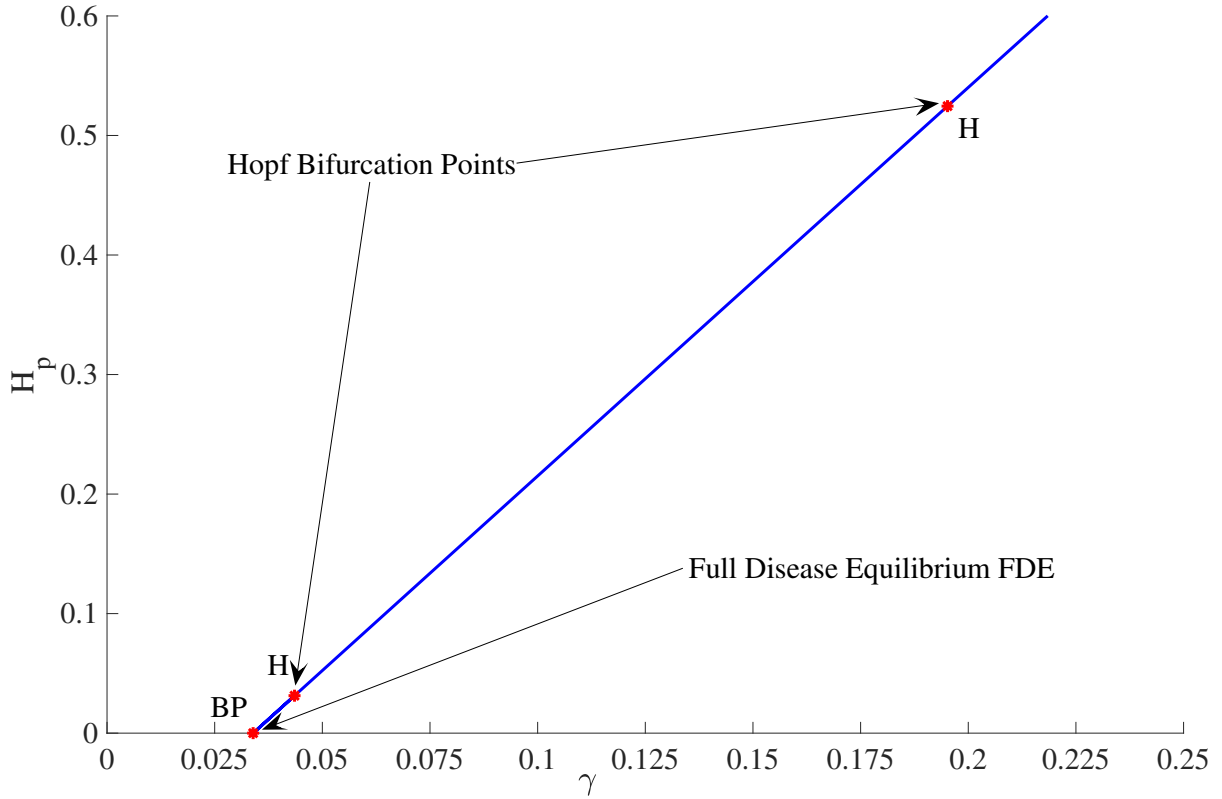


Figure 2: Bifurcation analysis made with MatCont - $k_p = 0.005$

planting, so that the harvest rate k_p ranges from $1.3/250$ to $1.8/250$, that is $k_p \in [0.0052, 0.0072]$ roughly. If the harvest starts later, say 500 days after planting, then $k_p \in [0.0026, 0.0036]$, so that we can choose the interval $[0.0025, 0.0072]$ for the harvesting rate in our model.

Last, but not least, the estimate of acquisition and inoculation rates is also another issue. Only two old studies have been done (see for instance [16]) on the transmission efficiency and it is in general very low (from 0.17% to 2%) for the vectors. Surprisingly, we didn't find information related to the number of plants visited by vectors, or the number of feeding bites, such that estimate of acquisition and inoculation rates is rather difficult. According to the literature, it seems that the transmission rate, from the infected vector to the susceptible host, β_{vp} , is rather low; in contrary, thanks to the fact that the feeding time is long (couple of hours), the inoculation rate from the infected plant to the susceptible vector, β_{pv} , can be high. Thus, without detailed information available in the literature, we will use the estimates of k_1 and k_2 given in [25], to estimate β_{vp} and β_{pv} . However, due to the fact that they have been estimated for individual plants and not for biomass we have to divide by the total biomass weight per square meter given above, since we consider a density of one individual per square meter. Thus $\beta_{vp} \in [0.0011, 0.0246]$, while for β_{pv} , we will not consider the same range, but a larger range, say $[0.0056, 0.23]$.

5.1 Sensitivity analysis of model (1)

To gain insight into the correct strategies for control of the crop vector-borne disease as described by model (1), we perform a sensitivity analysis.

The most important parameter is the basic reproduction number, \mathcal{J}_0 . In the current context it represents the amount of new infections per unit of plant biomass (vector) by the introduction of one unit of infected plant biomass (vector). In this section we aim to find out how the basic reproduction

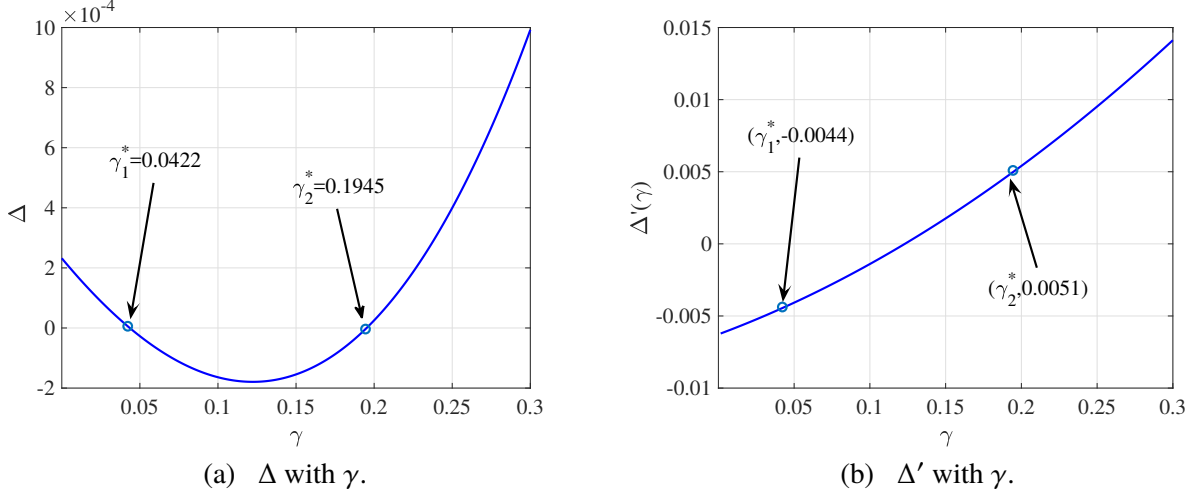


Figure 3: Illustration that the second Rough-Hurwitz condition can give imaginary eigenvalues ($k_p = 0.005$).

ratio respond to changes in the selected parameters. Mathematically, the sensitivity of \mathcal{J}_0 with respect to a parameter p is given by

$$\mathcal{F}_p^{\mathcal{J}_0} = \frac{\partial \mathcal{J}_0}{\partial p}.$$

However, we will consider the sensitivity index. This measures the change in \mathcal{J}_0 with respect to the percentage change in parameter p . The normalised sensitivity index of a variable \mathcal{J}_0 , that depends differentially on a parameter p , is defined as

$$\mathcal{E}_p^{\mathcal{J}_0} = \frac{\partial \mathcal{J}_0}{\partial p} \frac{p}{\mathcal{J}_0}.$$

The sensitivity index of \mathcal{J}_0 with respect to the parameter p is positive if \mathcal{J}_0 is increasing with respect to p and negative if \mathcal{J}_0 is decreasing with respect to p . For convenience, and following the discussion in Remark 3.4, we present the local sensitivity analysis on \mathcal{J}_0 . Straightforward calculation leads to the following results:

$$\begin{aligned} \mathcal{E}_r^{\mathcal{J}_0} &= \frac{\gamma r}{[(m_i - m_h)P^* + \gamma]P^*m_h(1 + \phi V^*)}, & \mathcal{E}_\phi^{\mathcal{J}_0} &= -\frac{\gamma \phi}{[(m_i - m_h)P^* + \gamma]P^*m_h(1 + \phi V^*)^2}, \\ \mathcal{E}_{k_p}^{\mathcal{J}_0} &= -\frac{\gamma \phi}{[(m_i - m_h)P^* + \gamma]P^*m_h}, & \mathcal{E}_{m_h}^{\mathcal{J}_0} &= -\frac{\gamma \phi (r_p(V^*) - k_p)}{[(m_i - m_h)P^* + \gamma]P^*m_h^2}, \\ \mathcal{E}_{m_i}^{\mathcal{J}_0} &= -\frac{P^*m_i}{(m_i - m_h)P^* + \gamma}, & \mathcal{E}_\alpha^{\mathcal{J}_0} &= \frac{\mu_1}{\mu_2 V^*}, & \mathcal{E}_{\mu_1}^{\mathcal{J}_0} &= -\frac{\mu_1}{\mu_2 V^*}, \\ \mathcal{E}_{\mu_2}^{\mathcal{J}_0} &= -1, & \mathcal{E}_{\beta_{p_v}}^{\mathcal{J}_0} &= 1, & \mathcal{E}_{\beta_{v_p}}^{\mathcal{J}_0} &= 1, \\ \mathcal{E}_\gamma^{\mathcal{J}_0} &= -\frac{\gamma}{(m_i - m_h)P^* + \gamma}. \end{aligned}$$

However, the sensitivity index gives us only partial information because we consider only the sensitivity for one parameter only and also only on \mathcal{J}_0 . We will now consider an additional sensitivity analysis considering that all parameters are changing. We will also focus on the system's variables H_p , I_p , S_v , and I_v . Using Table 1, page 7, we derive some global sensitivity analysis using two well-known methods: the eFast and the LHS-PRCC methods. The eFast method given in Fig.5, page 21, highlights first-order effects (main effects) and total effects (main and all interaction effects) of the parameters on the Model Outputs. We also derive a LHS-PRCC sensitivity analysis given in Fig.6, page 22. LHS-PRCC stands for Latin Hypercube Sampling and PRCC for Partial rank

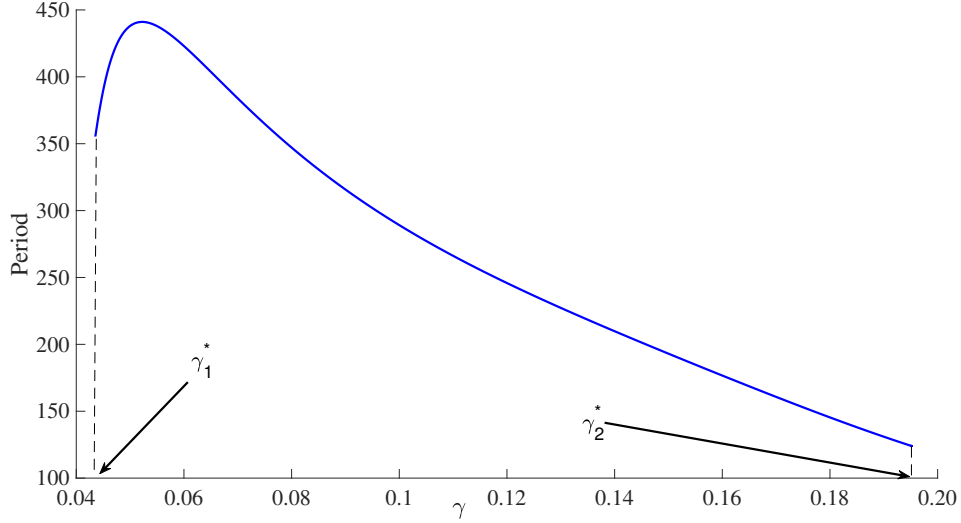


Figure 4: Period estimate of the periodic solution according to $\gamma \in [\gamma_1^*, \gamma_2^*]$, using MatCont, for $k_p = 0.005$.

correlation coefficient. These two methods give complementary information. Indeed the PRCC method provides mainly information about how the outputs are impacted if we increase (or decrease) the inputs of a specific parameter while the eFast indicates which parameter uncertainty has the greatest impact on the output variability (see for instance [35] for further explanations). Clearly here, the LHS-PRCC method provides the most interesting sensitivity analysis in terms of the contribution of each parameter, that may depend on the chosen variable. However, some parameters, related to the whiteflies dynamics (α_v , μ_2) or the transmission (β_{vp} and β_{pv} or the plant growth (r , ϕ , γ) may have a strong effect on the system dynamics. The values for the intervals used for the sensitivity analysis are given in Table 1, page 7.

In Figs. 7, page 23, and 8, page 24, we show the LHS-PRCC sensitivity analysis of both Basic reproduction numbers, \mathcal{R}_0 and \mathcal{J}_0 . Since they are mathematically equivalent, it make sense that their sensitivity analysis are almost similar. The results are in agreement with what we expect: when some parameters increase, then either \mathcal{R}_0 or \mathcal{J}_0 increases or decreases. The thresholds are more sensitive to some parameters, like β_{vp} , β_{pv} , r_p or ϕ . However, we can see that the roguing parameter, γ , has a strong negative effect, like k_p , the harvest rate. As we have seen earlier, very little is know about the values taken by β_{vp} and β_{pv} , such that additional studies would be welcome to conduct.

5.2 Numerical simulations

The above system of ordinary differential equations is highly nonlinear, hence in this section we present numerical simulations to support the results of the previous sections. In addition, we also present simulations to illustrate the model behavior with respect to the given parameters. We begin with the basic model where all parameters are chosen according to the base line values provided in Table 1, page 7. The system is integrated using MatLab's *ode solvers* and we adjust the solver's *RelTol* and *AbsTol* until the simulations have converged. The rest of the simulation were then performed using these baseline tolerance values.

The following simulations are done using parameters values given in Table 4, page 23, and chosen using Table 1, page 7.

In particular, when $\delta = 0$, Fig. 9, page 25, explores the impact of the roguing parameter, γ and also of \mathcal{R}_0 on the Healthy crop biomass, through the Hopf bifurcation. Thus, we consider either γ (Fig. 9(a)) or \mathcal{R}_0 (Fig. 9(b)) as bifurcation parameter and the vertical axis shows the values of the Healthy plant biomass. In Fig. 9 (a), an increase in γ , correspond to a large amount of healthy plant

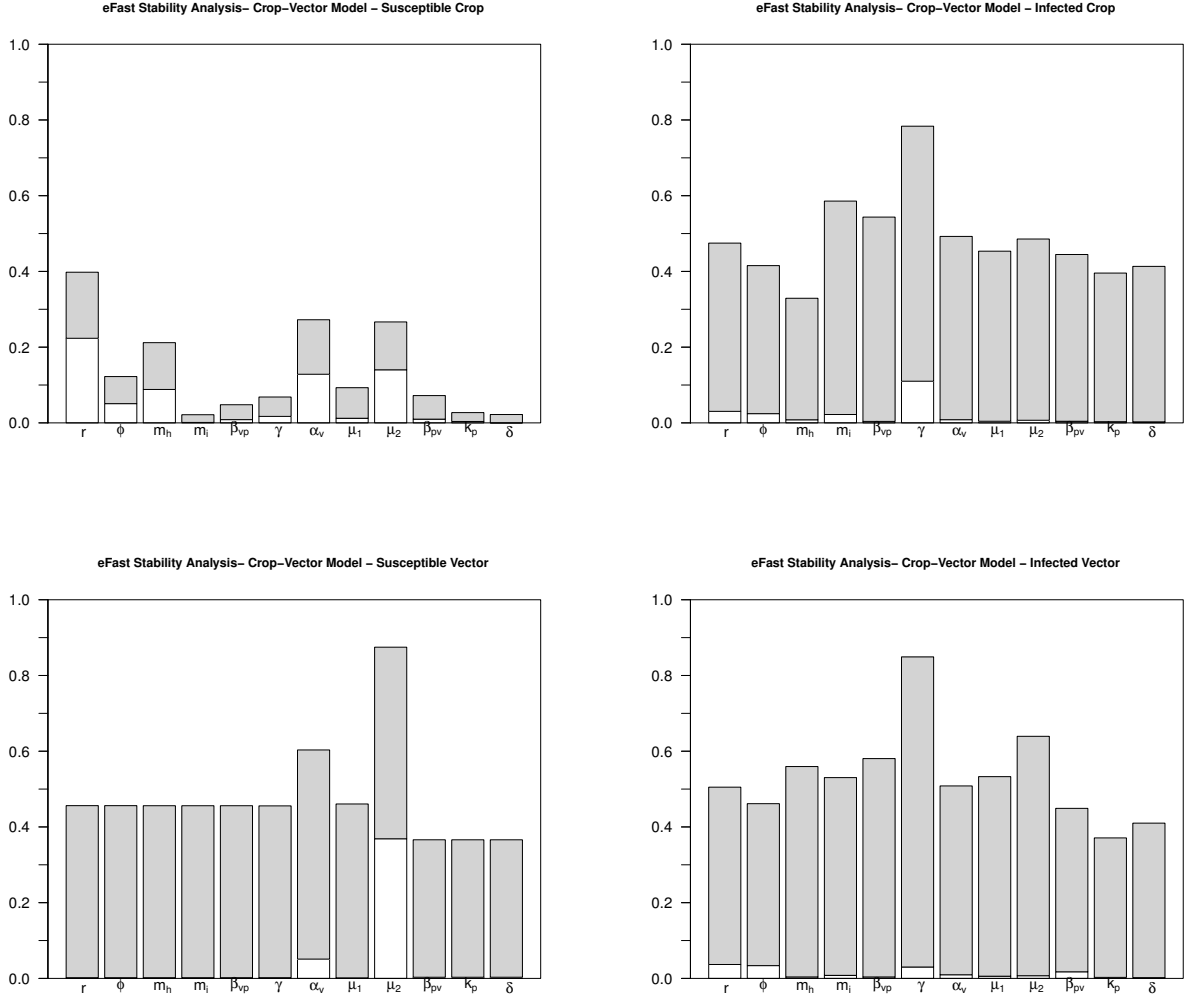


Figure 5: e-FAST Sensitivity analysis. White bar: first-order effects; Sum of white and grey bars: total effect.

biomass at equilibrium. Then, with \mathcal{R}_0 we obtain the opposite: when \mathcal{R}_0 is large, then $H_p = 0$ and the Full Disease equilibrium is reached.

Clearly, thanks to the plot of the stability function Δ in Fig. 3, the endemic equilibrium loses stability as \mathcal{R}_0 decreases when oscillatory solutions appear.

In Fig. 10, page 25, we provide the same simulations with $\delta > 0$, namely $\delta = 0.2$. Clearly, Hopf bifurcation occurs for smaller and larger values of γ , compared to the case when $\delta = 0$. In Fig. 11, page 26, we consider the case when $\delta \geq 0$, for a given value of γ , here 0.1, where Hopf bifurcation occurs. Here we need to solve the full system as given in (1). Interestingly, Matlab solvers struggled to solve the full system and adjustments of *RelTol* and *AbsTol* were again necessary. First, in Fig. 11, page 26, with (a), $\gamma = 0.1$, and (b), $\gamma = 0.2$, we show that the oscillatory behavior is amplified as δ grows. Thus $\delta > 0$ not only increases the interval, for γ , where Hopf bifurcation can take place, but also amplifies the amplitude of the oscillations. Last but not least, these numerical results confirm that our approach in the theoretical part, i.e. studying subsystem (10), page 12, was appropriate to show that a Hopf bifurcation can occur.

So far, roguing seems to be the best way to control the Cassava Mosaic Disease. However, as our study shows, roguing can amplify a possible periodic behavior in the system. It means that, at some

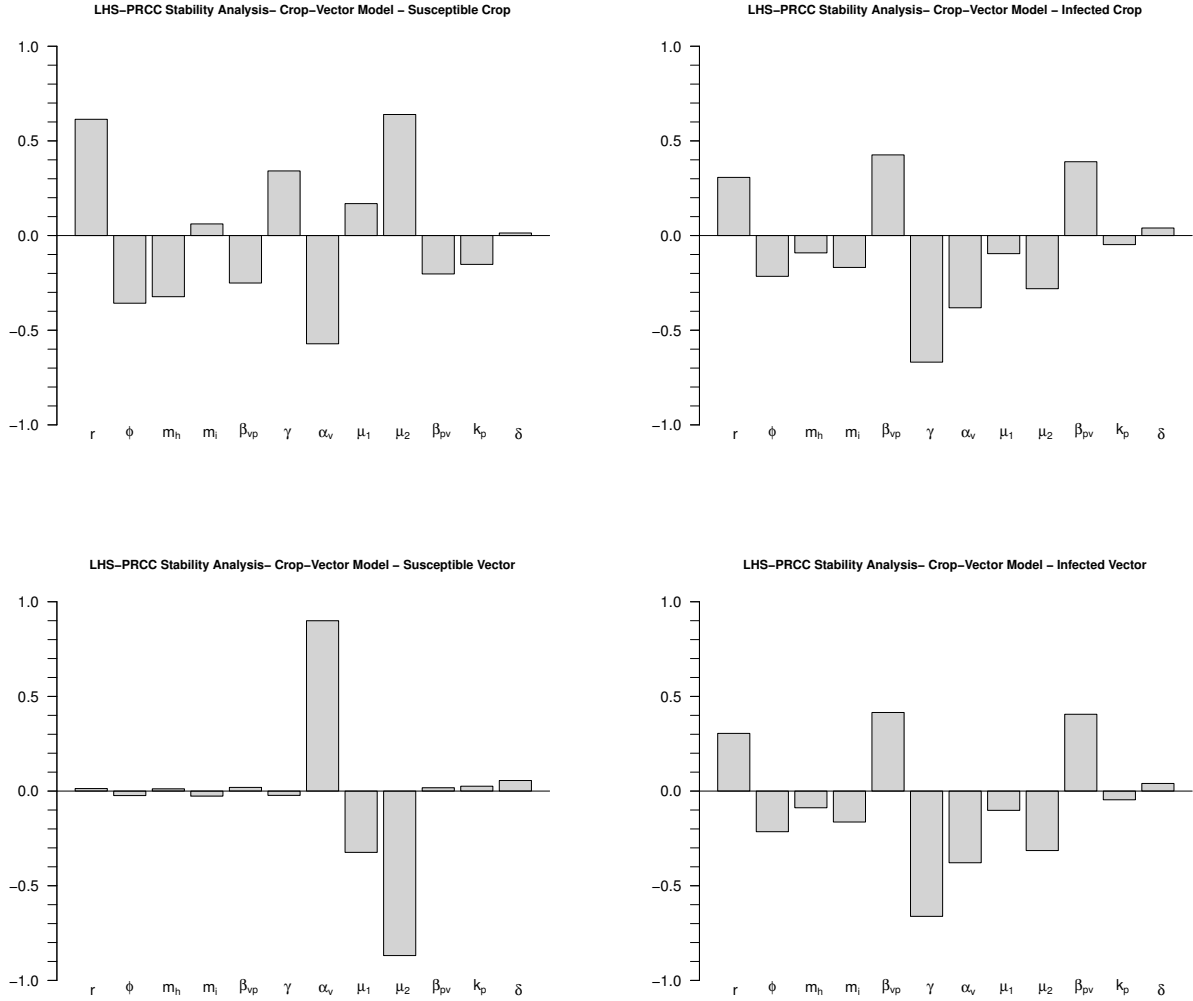


Figure 6: LHS-PRCC Sensitivity analysis.

moment, the disease seems to almost disappear, such the decision of stopping the roguing can be taken prematurely. Similar oscillatory behaviour has been observed in plant epidemiological models, see for example [44],[25]. However, it is important to notice that the model presented here is different from these works. In particular, their investigations are based on numerical simulations.

However, thanks to the sensitivity analysis provided in the previous subsection, some additional control strategies could be taken into account. For instance, reducing β_{vp} and β_{pv} is possible. In fact, in Kenya, tomato crops are protected against whiteflies using eco-friendly nets [38]. The results are very promising and this control approach seems to be suitable and also sustainable. However, the use of nets is only possible with young cassava plants, less than 1,5m high. The nets also may change locally the environmental parameters (temperature, humidity) of the plants, and thus may have an impact on their (photosynthetic) growth, and eventually, foster other kind of diseases, e.g., fungi. In fact, there exists several other control strategies, including the use of natural enemies, natural pesticides or pesticides extracted from plants, fungi like *Beauveria bassiana*, etc., and traps. Indeed, traps are widely used around the world, using pheromones or food to attract and catch insects (Anguelov et al., 2017a), and/or for mating disruption (Anguelov et al., 2017b).

Of course, additional bio-control strategies could be considered in our model: for examples, adding resistant plants (and find, like in [3], the right percentage of resistant cassava variety to plant to

LHS-PRCC Stability Analysis- Crop-Vector Model - R_0

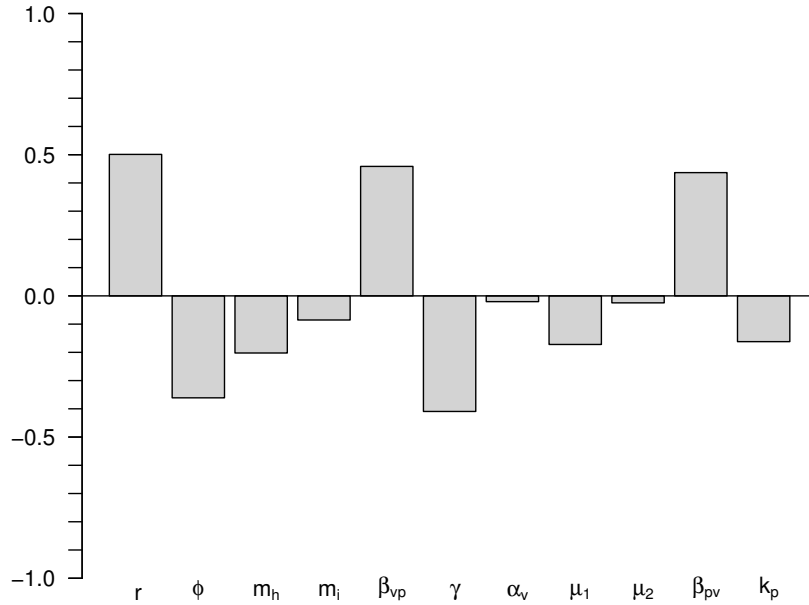


Figure 7: LHS-PRCC Sensitivity analysis of the Basic reproduction numbers \mathcal{R}_0 .

r	ϕ	m_h	m_i	β_{vp}	γ	α_v	δ	μ_1	μ_2	β_{pv}	k_p
0.04	0	0.01	0.01	0.008	[0, 1]	0.2	[0, 1]	0.12	0.0002	0.02	0.005

Table 4: Parameters values with $\delta \geq 0$.

reduce the impact of the disease), use entomopathogenic fungi or mycoinsecticides to kill whiteflies, etc. Last but not least, traps, using pheromones, either to catch the insects [1], and/or to disrupt mating [2]. In fact, they are many control strategies that could be tested using modeling and simulations, but also field experiments.

6 Conclusion

In this chapter, we presented a modeling example of a crop vector-borne disease with particular focus on cassava and the cassava mosaic virus disease. We showed that interesting mathematical models can be built that require various mathematical tools to be studied. Our model is relatively generic and could be applied to other plant-vector-virus interactions, and, of course, could be improved, taking into account vector aggregation and dispersal, like in [24], or include explicitly the spatial component, like in [9].

As alluded earlier, many other control measures may be used, but the proposed model suggests roguing is the most effective way to control the disease. This involves the uprooting of infected plants from the field. However, it has also been reported, see [32], that roguing is unpopular among farmers due to the resulting reduction in plant population. Our modeling effort suggests that the induced cycles may be misleading as the farmers may prematurely stop the roguing process.

In addition to roguing, it could be interesting to consider a proportion of a new variety of cassava, less susceptible to the virus or eventually resistant (like in [3]), and then estimate theoretically the

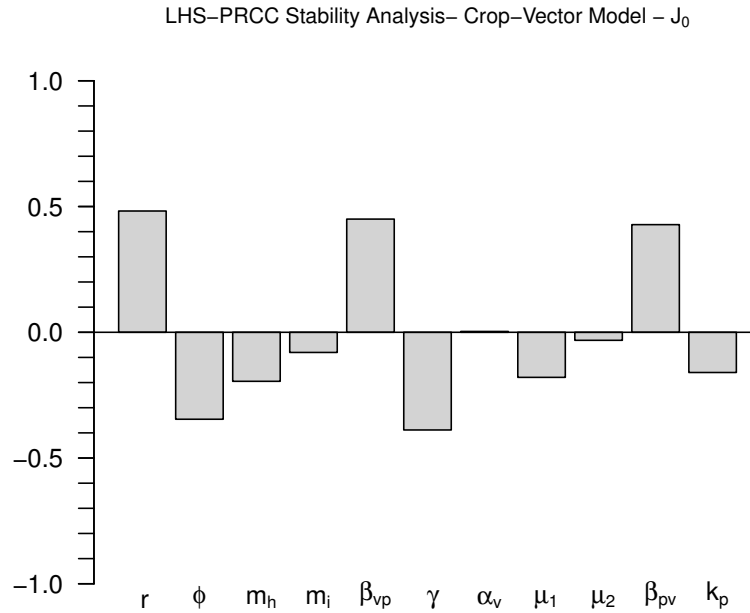


Figure 8: LHS-PRCC Sensitivity analysis of the Basic reproduction number \mathcal{J}_0 .

proportion needed, in a plot to reduce the epidemiological risk.

However, our interest is not only in the development and the study of new biological control models, but also in the questions highlighted by the modeling process, the analytical results and the numerical simulations. Indeed, despite a comprehensive literature review, various biological processes seem to be partially known, for instance, the transmission rates of the virus from the plant to the whitefly and from the whitefly to the plant. The plant biomass growth rates were only rigorously studied through experiments in Australia. Surprisingly, such rates were not estimated in Africa or South-America despite several projects on the production of several cassava varieties under various conditions. Certainly, these rates may change, in particular, for diseased plants (i.e., estimate for m_i), and for plants infested by susceptible whiteflies (i.e., estimate for ϕ). In contrast, very complex plant models have been calibrated, but only on healthy plants. However, the reader has to be aware that field experiments can be very difficult to conduct, sometimes with uncertainty in the outputs. That is why the use of models (even theoretical ones) can be useful in designing the appropriate experiments in order to feed the models and/or to improve the knowledge on the biological system. Models are not there to replace the field expert, but to support him/her in decision making. Last but not least, models can also help to test hypothesis about unknown processes and to focus on more specific experiments. However, whatever the models, it is always important to have in mind that they are only approximation of the reality, such that their predictability will always subject to some uncertainty.

We hope that this study on Cassava Mosaic Disease has highlighted some of the challenges to face when dealing with crop (vector-borne) diseases. That is why, to conclude, we strongly believe that crop diseases modeling can be a new field of research in Mathematical Epidemiology, and, more generally, in Applied Mathematics.

Acknowledgement The authors acknowledge the support of South African DST/NRF SARCHI Chair on Mathematical Models and Methods in Bioengineering and Biosciences (M3B2) of the

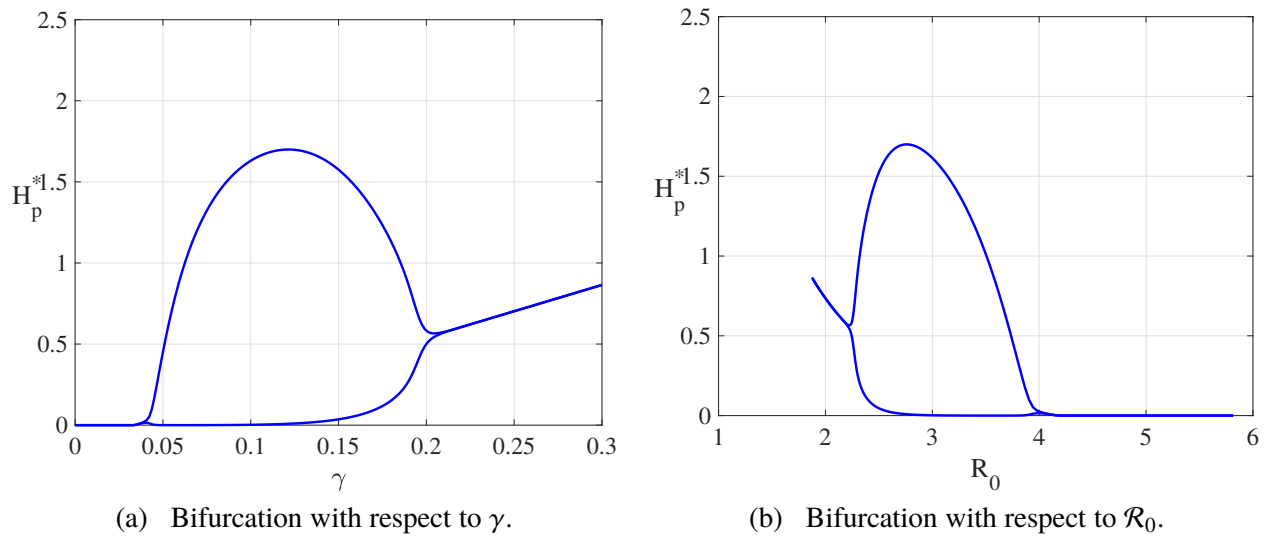


Figure 9: Bifurcation diagram showing the maxima and minima of Healthy plant biomass - $k_p = 0.005$.

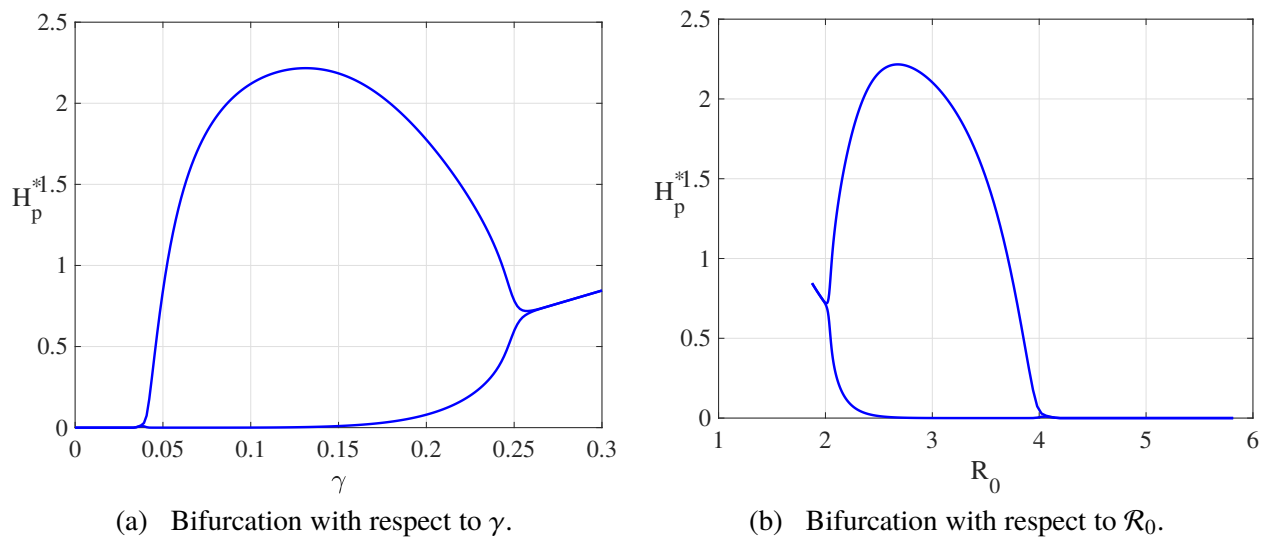


Figure 10: Bifurcation diagram showing the maxima and minima of Healthy plant biomass when $\delta = 0.2$

University of Pretoria (South Africa).

The authors thank the anonymous reviewers for their fruitful comments that greatly improve the initial manuscript.

References

- [1] Anguelov, R., Dufourd, C., Dumont, Y. Simulations and parameter estimation of a trap-insect model using a finite element approach. *Math. Comput. Simul.* **133**, 47–75 (2017).
- [2] Anguelov, R., Dufourd, C., Dumont, Y. Mathematical model for pest-insect control using mating disruption and trapping. *Appl. Math. Model.* **52**, 437–457 (2017).
- [3] Anguelov R., Lubuma J.M.-S. , Dumont Y. Mathematical analysis of vector-borne diseases on plants. In Guo, Y., Kang, M. Z., Dumont, Y. (Eds) *Plant growth modeling, simulation, visualization and applications. Proceedings PMA12 : The Fourth International Symposium on Plant Growth Modeling, Simulation, Visualization and Applications*, Shanghai, China, 31 October-3 November 2012. Beijing: IEEE Press, 22–29 (2012)

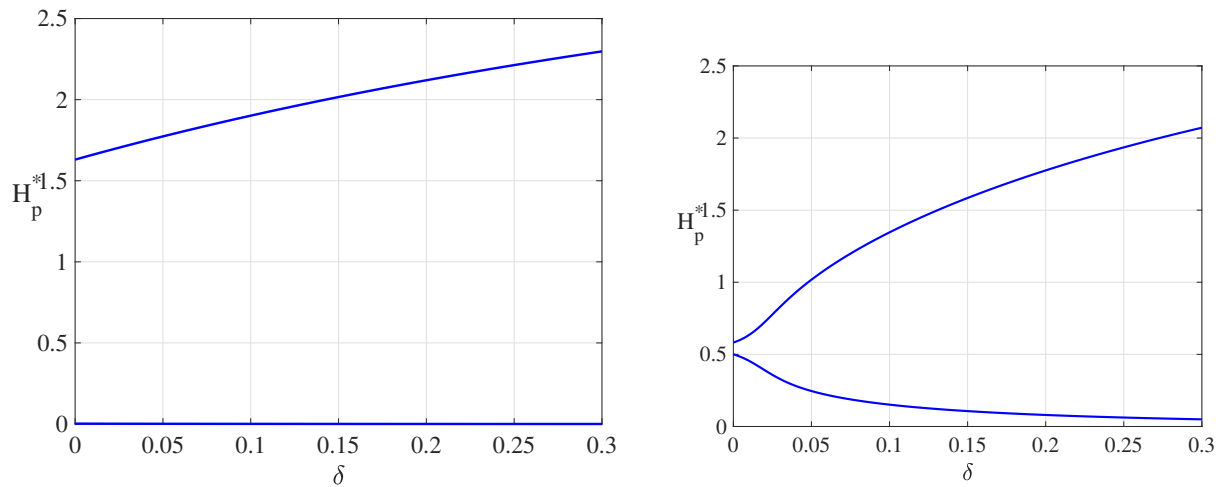


Figure 11: Bifurcation diagram showing the maxima and minima of Healthy plant biomass and Infected vector for different values of δ with $k_p = 0.005$ and (a) $\gamma = 0.1$ - (b) $\gamma = 0.2$.

- [4] Bacaër, N. A Short History of Mathematical Population Dynamics. Springer-Verlag London (2011).
- [5] Borkar, S. G., History of plant pathology, Agriculture series, Woodhead Publishing India Pvt Ltd, 248 pages (2017).
- [6] Busenberg S. and Cooke K. Vertically Transmitted Disease: Models and Dynamics, Springer-Verlag, Vol. 23 (1993)
- [7] F. Brauer. Mathematical epidemiology: Past, present, and future, Infectious Disease Modelling, 2(2): 113–127 (2017)
- [8] Castillo-Chavez, C., Feng, Z., Huang, W. On the computation of R_0 and its role on global stability, in: C. Castillo-Chavez, S. Blower, P. Van der Driessche, D. Kirschner, A.A. Yakubu (Eds.), Mathematical Approaches for Emerging and Reemerging Infectious Diseases, An Introduction, Springer: 229-250 (1998).
- [9] Chapwanya M. and Dumont Y. On crop vector-borne diseases. Impact of virus lifespan and contact rate on the traveling-wave speed of infective fronts, Ecological Complexity, **34**, 119–133 (2018).
- [10] Colvin, J., Omongo, C.A., Govindappa, M.R., Stevenson, P.C., Maruthi, M.N., Gibson, G., Seal, S.E., Muniyappa, V. Host-Plant Viral Infection Effects on Arthropod-Vector Population Growth, Development and Behaviour: Management and Epidemiological Implications. Advances in Virus Research, Academic Press **67**, 419–452 (2006).
- [11] Cushing, J.M. and Diekmann, O. The many guises of \mathcal{R}_0 (a didactic note). Journal of Theoretical Biology, **404**, 295–302 (2016).
- [12] Diekmann, O., Heesterbeek, J.A.P. and Roberts, M.G. The construction of next-generation matrices for compartmental epidemic models. Journal of the Royal Society Interface, **7**(47), 873–885 (2009).
- [13] Dhooge, A., Govaerts, W., Kuznetsov, Yu.A., Meijer, H.G.E., Sautois, B. New features of the software MatCont for bifurcation analysis of dynamical systems. MCMDS **14**(2) 147–175 (2008).
- [14] Food and Agriculture Organization of the United Nations (FAO): Save and Grow: Cassava. A Guide to Sustainable Production Intensification. Rome (2013).
- [15] Fargette, D. Epidemiologie de la mosaïque Africaine du manioc en Côte d’Ivoire. PhD thesis. pp 203. Science and Technology University, Montpellier, (1985).
- [16] Fargette, D., Fauquet, C., Grenier, E., Thresh, J. M. The spread of African cassava mosaic virus into an within cassava fields, Journal of phytopathology **130**(4): 289–302 (1990).

- [17] Fargette, D., and Vie, K. Modeling the temporal primary spread of African cassava mosaic virus into plantings. *Phytopathology* **84**(4), 378–382 (1994).
- [18] Fauquet Claude, and Fargette Denis. African Cassava Mosaic Virus: Etiology, Epidemiology and Control, *Plant Disease* **74**(6): 404–11 (1990).
- [19] Gabriel, L.F., Streck, N.A., Roberti, D.R., Chielle, Z.G., Uhlmann, L.O., da Silva, M.R., and da Silva, S.D. Simulating cassava growth and yield under potential conditions in Southern Brazil. *Agronomy Journal* **106**(4): 1119–1137 (2014).
- [20] Gilligann C.A. An epidemiological framework for disease management, *Advances in Botanical Research* **38**, 2–65 (2002).
- [21] Goodman, M.M., and Galinat, W.C. The history and evolution of Maize, *Critical Reviews in Plant Sciences*, **7:3**, 197–220 (1988).
- [22] Guckenheimer, J., and Holmes, P. *Nonlinear Oscillations, Dynamical Systems, and Bifurcations of Vector Fields*, Springer (2002).
- [23] Hawkes J.G., and Francisco-Ortega J. The early history of the potato in Europe. *Euphytica* **70**:1–7 (1993).
- [24] Hebert, M.P., Allen, L.J.S. Disease outbreaks in plant-vector-virus models with vector aggregation and dispersal. *Discrete & Continuous Dynamical Systems - B*, **21**(7) : 2169-2191 (2016).
- [25] Holt, J., Jeger, M.J., Thresh, J.M., Otim-Nape, G.W. An epidemiological model incorporating vector population dynamics applied to African cassava mosaic virus disease. *Journal of Applied Ecology* **34**, 793–806 (1997).
- [26] Isendahl, C. The Domestication and Early Spread of Manioc (*Manihot Esculenta* Crantz): A Brief Synthesis. *Latin American Antiquity*, **22**(4), 452–468 (2011)
- [27] Jeger, M.J., Holt J., van den Bosch, F., Madden L.V. Epidemiology of insect-transmitted plant viruses: modelling disease dynamics and control interventions. *Physiological Entomology* **29**, 291–304 (2004).
- [28] Jeger, M. J., Madden, L. V., and van den Bosch, F. Plant Virus Epidemiology: Applications and Prospects for Mathematical Modeling and Analysis to Improve Understanding and Disease Control. *Plant Disease* **102**(5), 837–854 (2018).
- [29] Keating, B.A., Evenson, J.P., and Fukai, S. Environmental effects on growth and development of cassava (*Manihot esculenta* Crantz.) II. Crop growth rate and biomass yield, *Field Crops Research*, **5**, 283–292 (1982).
- [30] Kuznetsov, Yu. A. *Elements of Applied Bifurcation Theory*, Springer-Verlag. (third edition 2004) (1998).
- [31] Lebon, A., Mailleret, L., Dumont, Y., Grogard, F. Direct and apparent compensation in plant–herbivore interactions, *Ecological Modelling* **290**, 192–203, (2014).
- [32] Legg J.P., Lava Kumar P., Makesh Kumar T., Tripathi L., Ferguson M., Kanju E., Ntawuruhunga P., Cuellar W. Cassava virus diseases: biology, epidemiology, and management. *Advances in Virus Research*, **91**, 85–142 (2015).
- [33] Lucas, G.B., Campbell, C.L., Lucas, L.T. History of Plant Pathology, in *Introduction to Plant Diseases: Identification and Management*, Springer US, Boston (MA), 15–19 (1992).
- [34] Macfayden, S., Paull, C.A., Boykin, L.M., Barro, P.J., Maruthi, M.N., Otim, M.H., Kalyebi, A., Vassallo, D.G., Sseruwagi, P., Tay, W.T., Delatte, H., Seguni, Z.S., Colvin, J., Omongo, C. Cassava whitefly, *Bemisia tabaci* (Gennadius) (Hemiptera: Aleyrodidae) in East African farming landscapes: a review of the factors determining abundance. *Bulletin of Entomological Research*, **108**(5), 565–582 (2018).
- [35] Marino S., Hogue I.B., Ray C.J., Kirschner D.E. A methodology for performing global uncertainty and sensitivity analysis in systems biology. *Journal of Theoretical Biology* **254**(1), 178–196 (2008).

- [36] Maruthi, M. N., Colvin, J., Seal, S., Thresh, J. M. First report of a district begomovirus infecting cassava in Zanzibar. *Plant Disease* **86**, 187 (2002).
- [37] Matthews, R.B., Hunt, L.A. GUMCAS: a model describing the growth of cassava (*Manihot esculenta* L. Crantz), *Field Crops Research* **36**(1), 69–84 (1994).
- [38] Mutisya, S., Saidi, M., Opiyo, A., Ngouajio, M., Martin, T. Synergistic effects of agronet covers and companion cropping on reducing whitefly infestation and improving yield of open field-grown tomatoes. *Agronomy (Basel)* **6** (42), 14 p (2016)
- [39] Nelson, S. Sooty Mold. Plant Disease PD-52. Mānoa, Honolulu, Hawaiï, Cooperative extension Service, College of Tropical Agriculture and Human Resources, University of Hawaii (2008).
- [40] Paine, C. E., Marthews, T. R., Vogt, D. R., Purves, D. , Rees, M. , Hector, A. and Turnbull, L. A. How to fit nonlinear plant growth models and calculate growth rates: an update for ecologists. *Methods in Ecology and Evolution* **3**: 245–256 (2012)
- [41] Patil, B. L. and Fauquet, C. M. Cassava mosaic geminiviruses: actual knowledge and perspectives. *Molecular Plant Pathology* **10**, 685–701 (2009).
- [42] Tironi, L. F., Streck, N. A., Gubiani, P. I., Benedetti, R. P., Freitas, C. P. O. Simanihot: A process-based model for simulating growth, development and productivity of cassava. *Engenharia Agrícola*, **37**(4), 471–482 (2017).
- [43] Tresh, J.M. , Cooter, R.J. Strategies for controlling cassava mosaic virus disease in Africa. *Plant Pathology* **54**, 587–614 (2008).
- [44] van den Bosch, F., and de Roos, A. M. (1996). The dynamics of infectious diseases in orchards with roguing and replanting as control strategy. *Journal of Mathematical Biology*, **35**(2), 129-157.
- [45] Van den Driessche, P. and Watmough, J. Reproduction numbers and sub-threshold endemic equilibria for compartmental models of disease transmission. *Mathematical Biosciences*, **180**(1-2), 29–48 (2002).
- [46] Waltman, P. *A Second Course in Elementary Differential Equations*, Dover, New York (2004).
- [47] Yasada T. and Yoshida H. Coefficient criterion for four-dimensional Hopf bifurcations: a complete mathematical characterisation and applications to economic dynamics. *Chaos, Solitons and Fractals*, **18**, 525–536 (2003).
- [48] Zhang, X. , Holt, J. and Colvin, J. A general model of plant virus disease infection incorporating vector aggregation. *Plant Pathology* **49**: 435–444 (2000).

7 Annexe A

7.1 Existence of a full endemic equilibrium for model (1)

To determine the endemic equilibria, we have to solve the following system

$$\begin{cases} \frac{r_p H_p^\#}{1 + \phi V^\#} - m_h H_p^\# P^\# - \beta_{vp} H_p^\# I_v^\# - k_p H_p^\# = 0, \\ \frac{r_p I_p^\#}{1 + \phi V^\#} + \beta_{vp} H_p^\# I_v^\# - m_i P^\# I_p^\# - (\gamma + k_p) I_p^\# = 0, \\ \alpha_v \left(1 + \delta \frac{I_p^\#}{1 + I_p^\#} \right) V^\# - (\mu_1 + \mu_2 V^\#) S_v^\# - \beta_{pv} S_v^\# I_p^\# = 0, \\ \beta_{pv} S_v^\# I_p^\# - (\mu_1 + \mu_2 V^\#) I_v^\# = 0, \end{cases} \quad (19)$$

where the $^\#$ denote the value at equilibrium. However we can study different cases, like $H_p^\# > 0$ and, in particular, $H_p^\# = 0$, corresponding to the Full Disease Equilibrium, FDE.

Thus, assuming $H_p^\# = 0$ leads to

$$P^\# = I_p^\# = \frac{1}{m_i} \left(\frac{r}{1 + \phi V^\#} - (\gamma + k_p) \right),$$

with

$$V^\# = \frac{1}{\mu_2} \left(\alpha_v \left(1 + \delta \frac{I_p^\#}{1 + I_p^\#} \right) - \mu_1 \right) \quad (20)$$

Thus using (19)₂, we deduce

$$m_i I_p^\# + (\gamma + k_p) = \frac{r \mu_2 (1 + I_p^\#)}{1 + \phi V^\#} = \frac{r \mu_2 (1 + I_p^\#)}{\mu_2 (1 + I_p^\#) + \phi (\alpha_v (1 + I_p^\# + \delta I_p^\#) - \mu_1 (1 + I_p^\#))}.$$

Reducing to the same denominator, we derive

$$\left(m_i I_p^\# + (\gamma + k_p) \right) \left((1 + I_p^\#) (\mu_2 + \phi (\alpha_v - \mu_1)) + \delta \phi \alpha_v I_p^\# \right) = r \mu_2 (1 + I_p^\#),$$

that is

$$\left(m_i I_p^\# + (\gamma + k_p) \right) \left((\mu_2 + \phi (\alpha_v - \mu_1)) + (\mu_2 + \phi (\alpha_v - \mu_1) + \delta \phi \alpha_v) I_p^\# \right) = r \mu_2 (1 + I_p^\#).$$

Expanding all terms in the previous equality, we obtain a second order equation

$$\begin{aligned} & (m_i (\mu_2 + \phi (\alpha_v - \mu_1)) + (\gamma + k_p) (\delta \phi \alpha_v + (\mu_2 + \phi (\alpha_v - \mu_1))) - r \mu_2) I_p^\# + \\ & + m_i ((\mu_2 + \phi (\alpha_v - \mu_1) + \delta \phi \alpha_v)) (I_p^\#)^2 + ((\gamma + k_p) (\mu_2 + \phi \alpha_v - \mu_1) - r \mu_2) = 0 \end{aligned}$$

That is

$$(B + \delta m_i \phi \alpha_v) (I_p^\#)^2 + (B + A + (\gamma + k_p) \phi \alpha_v \delta) I_p^\# + A = 0,$$

with

$$A = (\gamma + k_p) (\mu_2 + \phi (\alpha_v - \mu_1)) - r \mu_2 = \phi (\gamma + k_p) (\alpha_v - \mu_1) - (r - (\gamma + k_p)) \mu_2,$$

$$B = m_i (\mu_2 + \phi (\alpha_v - \mu_1)) > 0.$$

Assuming

$$\frac{(\gamma + k_p) (\mu_2 + \phi (\alpha_v - \mu_1))}{r \mu_2} < 1,$$

then $A < 0$. Then, we compute

$$\Delta = (B + A + (\gamma + k_p) \phi \alpha_v \delta)^2 - 4A(B + \delta m_i \phi \alpha_v) > 0,$$

such that, we deduce the following real positive root

$$I_p^\# = \frac{1}{2(B + \delta m_i \phi \alpha_v)} \left(- (B + A + (\gamma + k_p) \phi \alpha_v \delta) + \sqrt{\Delta} \right) > 0. \quad (21)$$

Since we always assume that $r > \gamma + k_p$, we can consider the following two cases:

- when $\phi = 0$ (no impact of the vectors on the plant growth rate), FDE always exists. Using (21), we deduce

$$I_p^\# = \frac{-A}{B} = \frac{r_p - (\gamma + k_p)}{m_i} > 0.$$

Then, the other values $V^\#$ (using (20)), $S_v^\#$ (using (19₃)), and $I_v^\#$ follow.

- When $\phi > 0$ and such that

$$\phi < \frac{(r_p - (\gamma + k_p)) \mu_2}{(\gamma + k_p) (\alpha_v - \mu_1)}, \quad (22)$$

then, according to (21), FDE always exists .